

*He alone is my rock and my salvation;
He is my fortress, I will never be shaken*

Psalm 62:2

University of Alberta

An Investigation into the Synthesis and Tunability of Copper (I) Compounds

by

Lydia A M Glover

A thesis submitted to the Faculty of Graduate Studies and Research
in partial fulfillment of the requirements for the degree of

Master of Science

Department of Chemistry

©Lydia Annette Marie Glover

Fall 2012

Edmonton, Alberta

Permission is hereby granted to the University of Alberta Libraries to reproduce single copies of this thesis and to lend or sell such copies for private, scholarly or scientific research purposes only. Where the thesis is converted to, or otherwise made available in digital form, the University of Alberta will advise potential users of the thesis of these terms.

The author reserves all other publication and other rights in association with the copyright in the thesis and, except as herein before provided, neither the thesis nor any substantial portion thereof may be printed or otherwise reproduced in any material form whatsoever without the author's prior written permission.

Abstract

The bis(diphenyltrimethylsilyliminophosphorano)methanediide ligand has shown exemplary reactivity in forming a variety of useful pincer, chelate, monomeric and bimetallic bridged metal complexes. The methanediide ligand reactivity varies greatly with regard to many factors including the choice and quantity of metal precursor. Research has recently demonstrated the formation of novel boat-shaped hexacopper clusters, with alkyl, halide and oxide bridges, and an anionic tri-lithiated complex with a copper (I) dichloride counter-cation. In addition to the novelty of forming various copper compounds is the necessity for exploration of their usefulness as materials specifically, exploitation of their luminescent and catalytic properties. The hexacopper clusters of concern in this study all exhibit photoluminescence in the visible spectral region whose maximum wavelength depends on the capping ligand. A detailed discussion of the reactivity exhibited by the bis(diphenyltrimethylsilyliminophosphorano)methanediide ligand with specific focus on the synthesis of a series of copper complexes and their notable luminescent, reduction-oxidation and electronic properties will be presented.

Acknowledgements

My acknowledgements start with a big thank you to the University of Alberta: without this organization I wouldn't where I am. This includes all of the faculty members, support staff and students who make the experiences learned here memorable and possible.

A special thank you must go out to Dr. Ron Cavell for allowing me to take on his research ideas and taking me on as his only student. Thank you for an entire lab all to myself to allow my scientific creativity to flow. Some of the best advice, with regard to my research, came from Dr. Guibin Ma. Thank you for teaching me techniques and methods pertinent to the research and allowing me to take the lead on projects.

Dr. Jon Veinot was not only my supervisor but also a mentor to me. For over six years you have been there for me, pushing and supporting me throughout the years. Be it personal or professional you have been so great, thank you so much.

Thank you Veinot Group! Everyone in the Veinot group has been kind to me from undergrad to graduate studies. You all are great fun. A special thank you must go out to those who offered assistance with editing and motivation with regard to the completion of this thesis, especially Mita Dasog and Sarah Regli. One specific lab member is so much more than a lab member, thank you Brenna Brown, through the laughter and the tears you have been a great friend. Seven years and still going strong! Thank you very much to ALL my friends who

offered so much support in their own unique ways, I hope you all know how much it means to me.

My family is my life; they are and will always be my cheering section. Thank you for all the lessons you taught me and for giving me the drive to finish everything I start, making sure to mind the details. I love you Mom and Dad (Lucie & Serge) and Gabrielle! And everyone knows that's not the end of my family, thank you Grandma, Grandpa, Sylvain, Alain, Yvette, Joséé and France.

Lastly, a huge thank you goes to my number one fan, my husband, Bob Glover. You have been nothing short of amazing in your dedication to me. Thank you for your support through this journey, we made it. I'll love you today, tomorrow, always.

Table of Contents

Chapter 1: From Carbon, to Complexes, To Catalysis and Onwards to Copper

<i>1.1</i>	<i>Carbon, the Element</i>	<i>2</i>
<i>1.2</i>	<i>Fischer, Schrock and Geminal Dianions</i>	<i>3</i>
<i>1.2.1</i>	<i>Fischer Carbenes</i>	<i>4</i>
<i>1.2.2</i>	<i>Schrock Carbenes</i>	<i>4</i>
<i>1.2.3</i>	<i>Geminal Carbenes</i>	<i>4</i>
<i>1.3</i>	<i>Origin of the Pincer</i>	<i>5</i>
<i>1.3.1</i>	<i>Pincers: From the Battlefield to the Laboratory</i>	<i>6</i>
<i>1.4</i>	<i>Ligand Design</i>	<i>7</i>
<i>1.4.1</i>	<i>Steric Effects on Ligand Design</i>	<i>8</i>
<i>1.4.2</i>	<i>Nitrogen Versus Phosphorus</i>	<i>10</i>
<i>1.5</i>	<i>Pincers and Catalysis</i>	<i>11</i>
<i>1.5.1</i>	<i>The Big Catalysis Players: Heck, Sonogashira and Suzuki</i>	<i>11</i>
<i>1.5.2</i>	<i>Unsymmetric Pincer Ligands</i>	<i>14</i>
<i>1.5.3</i>	<i>Asymmetric Pincer Ligands</i>	<i>15</i>
<i>1.6</i>	<i>Bis(diphenyltrimethylsilyliminophosphorano)methane</i>	<i>16</i>
<i>1.6.1</i>	<i>Reactions of Compound 1</i>	<i>17</i>
<i>1.6.2</i>	<i>Recent Reactions of Compound 1</i>	<i>19</i>
<i>1.7</i>	<i>Copper as a Catalyst</i>	<i>21</i>
<i>1.7.1</i>	<i>Cross-Coupling Reactions: Further Investigation on the Ullmann Reaction</i>	<i>22</i>

1.7.2	<i>Cross-Coupling Reactions: Beyond the Ullmann reaction</i>	23
1.7.3	<i>Copper Catalysts: New Directions</i>	24
1.8	<i>Thesis Outline</i>	26
1.9	<i>References</i>	27

Chapter 2: The Synthesis of Hexanuclear Copper Clusters

2.1	<i>The Basics of Copper</i>	33
2.2	<i>Copper (I)</i>	33
2.3	<i>Copper Click Reactions</i>	34
2.4	<i>The Bis(diphenyltrimethylsilyliminophosphorano)methanediide Ligand System</i>	35
2.4.1	<i>Computational Analysis of 1</i>	36
2.4.2	<i>Sulfur-based pincer ligands</i>	38
2.5	<i>Reactions of 1</i>	38
2.6	<i>Experimental</i>	43
2.6.1	<i>Materials:</i>	43
2.6.2	<i>General Methods:</i>	43
2.6.3	<i>Synthetic Procedures:</i>	44
2.7	<i>Results and Discussion</i>	50
2.7.1	<i>Copper reactions with Li₂L</i>	50
2.7.2	<i>Photoluminescent Properties of Hexanuclear Copper Clusters</i>	54

2.7.3	<i>Photoluminescent Properties of Hexanuclear Copper Clusters Beyond Halides</i>	58
2.7.4	<i>Electrochemical Analysis of the Ligands and the Hexanuclear Copper Clusters</i>	59
2.8	<i>Conclusions</i>	66
2.9	<i>References</i>	68

Chapter 3: The Formation of a Tri-lithium

Bis(iminodiphenylphosphorano)methanide Copper (I) Dichloride

3.1	<i>Introduction</i>	75
3.1.1	<i>Catalytic Properties</i>	75
3.1.2	<i>Optical Properties</i>	76
3.1.3	<i>The Original Goal: Copper as a Sensor and/or Catalyst</i>	77
3.2	<i>Experimental</i>	79
3.2.1	<i>Materials:</i>	79
3.2.2	<i>General Methods:</i>	79
3.2.3	<i>Synthetic Procedure:</i>	80
3.3	<i>Results and Discussion</i>	81
3.4	<i>Conclusions</i>	89
3.5	<i>References</i>	90

Chapter 4: Conclusions and Future Work

4.1	<i>Conclusions</i>	94
4.2	<i>Future Work</i>	95

4.3	<i>References</i>	94
------------	-------------------	----

Appendix A1: Crystal Structure Determination

A1:	<i>Crystal Structure Determination</i>	96
------------	--	----

List of Tables

<i>Table 3.1</i>	<i>Attempted reactions for the formation of hexanuclear copper clusters with chalcogenide caps</i>	83
<i>Table A1.1</i>	<i>Selected bond lengths (Å): Structure A</i>	102
<i>Table A1.2</i>	<i>Selected bond lengths (Å): Structure B</i>	102
<i>Table A1.3</i>	<i>Selected bond angles (°) Structures A & B</i>	103

List of Figures

Figure 1.1	Types of metal carbene species	3
Figure 1.2	Battle of Cannae during the Second Punic war depicting the pincer maneuver attack tactic	6
Figure 1.3	PCP-pincer backbone ligands: (a) alkyl, (b) aryl and (c) cycloheptatirenyl ligand	8
Figure 1.4	Equilibrium between carbene and olefin complexes, achieved through α -H- and β -H-elimination, respectively	9
Figure 1.5	(a) NCN pincer complex (b) PCP pincer complex, with palladium metal centres, used as catalysts for Heck, Sonogashira and Suzuki reactions	12
Figure 1.6	CNC reusable pincer for Suzuki reactions	13
Figure 1.7	Unsymmetrical PCN pincers used for various cross-coupling reactions	14
Figure 1.8	Palladium-based chiral pincer catalysts for condensation reactions	15
Figure 1.9	Bis(diphenyltrimethylsilyliminophosphorano)methane	16
Figure 1.10	ORTEP representation of $\text{NiCl}_2[\text{CH}_2(\text{PPh}_2=\text{NSiMe}_3)_2]$. Thermal ellipsoids drawn at the 50% probability level (carbon atoms of phenyl rings are of arbitrary radius)	18
Figure 1.11	Left: ORTEP image of $[\text{Zr}\{\text{C}(\text{Ph}_2\text{P}=\text{NAd})_2-\kappa^3\text{C},\kappa\text{N},\kappa\text{N}\}\{\text{CH}_2\text{Ph}\}_2]$ Right: ORTEP image of $[\text{Li}\{\text{HC}(\text{Cy}_2\text{P}=\text{NSiMe}_3)_2-\kappa\text{C},\kappa\text{N},\kappa\text{N}\}\{\text{OEt}_2\}]$, atoms are represented by Gaussian ellipsoids at the 20% probability level	19
Figure 1.12	Bis[hydrotris(3-methyl-imidazolin-2-ylidene-1-yl)borate]tricopper(I) tetrafluoroborate	24
Figure 2.1	Canadian Parliament building. Left image: prior to restoration, right image: post restoration	33
Figure 2.2	Dinuclear copper (I) complex $[\text{Cu}^{\text{I}}(\text{L-L})\text{Cu}^{\text{I}}]^{2+}$ ($\text{L} = [\text{N}-(2\text{-mercaptopyrpyl})-\text{N},\text{N}-\text{bis}(2\text{-pyridylmethyl})\text{amine}]$) used in CO_2 sequestering	34

Figure 2.3	ORTEP view of $[Li_2C(P=NSi(CH_3)_3)_2]_2$, hydrogen atoms, methyl carbon atoms attached to the silicon atoms and the phenyl carbons, except the ipso-carbons have been omitted for clarity. Ellipsoids are presented at a 20% probability level	36
Figure 2.4	ORTEP crystal structure representations of (a) $[TiCl_2\{C(Ph_2P=NSiMe_3)_2-\kappa^3C,N,N'\}]$ and (b) $[HfCl_2\{C(Cy_2P=NSiMe_3)_2-\kappa^3C,N,N'\}]$, illustrating the isostructures. Hydrogen atoms, methyl carbon atoms attached to the silicon atoms and the phenyl carbons, except the ipso-carbons have been removed for clarity	40
Figure 2.5	ORTEP representation of $[(\eta^4-cod)Pt\{C(Ph_2P=NSiMe_3)_2-\kappa C,\kappa N\}]$. Hydrogen atoms, methyl carbon atoms attached to the silicon atoms and the phenyl carbons, except the ipso-carbons have been removed for clarity	41
Figure 2.6	Distorted hexanuclear copper cluster for the determination of copper (II) ions	52
Figure 2.7	Core structures of the hexanuclear copper clusters (3) left, (4) middle and (5) right	53
Figure 2.8	UV-Visible absorbance spectra for compounds: (3) $[Cu_6Cl_2((C_6H_5)_2P=NSi(CH_3)_3)_2]_2$, (4) $[Cu_6Br_2((C_6H_5)_2P=NSi(CH_3)_3)_2]_2$, (5) $[Cu_6I_2((C_6H_5)_2P=NSi(CH_3)_3)_2]_2$, (7) $[CuI(C_6H_5)_2P=NSi(CH_3)_3]_2$, and (8) $[Cu_6(CH_3)_2((C_6H_5)_2P=NSi(CH_3)_3)_2]_2$	55
Figure 2.9	Photoluminescence emission spectra for compounds: (3) $[Cu_6Cl_2((C_6H_5)_2P=NSi(CH_3)_3)_2]_2$, (4) $[Cu_6Br_2((C_6H_5)_2P=NSi(CH_3)_3)_2]_2$, (5) $[Cu_6I_2((C_6H_5)_2P=NSi(CH_3)_3)_2]_2$, (7) $[CuI(C_6H_5)_2P=NSi(CH_3)_3]_2$, and (8) $[Cu_6(CH_3)_2((C_6H_5)_2P=NSi(CH_3)_3)_2]_2$. Excitation was done through a 325 nm He-Cd laser	58
Figure 2.10	Aluminum catalyst for olefin polymerization $[\kappa C,\kappa C,\kappa N,\kappa N'-\{(Me_3SiN=P(Ph)_2)_2C\}(Me_2Al)_2]$	60
Figure 2.11	Cyclic voltammogram of 1 in dry, deaerated	61

acetonitrile and 0.1 M tetrabutyl ammonium perchlorate as supporting electrolyte at a scan rate of 50 mV/s at 25°C. Standardized to Fc^+/Fc

- Figure 2.12** Cyclic voltammogram of compound 2 in dry acetonitrile and 0.1 M tetrabutyl ammonium perchlorate as supporting electrolyte at a scan rate of 50 mV/s at 25°C. Standardized to Fc^+/Fc 61
- Figure 2.13** Cyclic voltammogram of 3 in dry acetonitrile and 0.1 M tetrabutyl ammonium perchlorate as supporting electrolyte at a scan rate of 50 mV/s at 25°C. Standardized to Fc^+/Fc . a) reductive cycle b) oxidative cycle 63
- Figure 2.14** Cyclic voltammogram of 4 in dry acetonitrile and 0.1 M tetrabutyl ammonium perchlorate as supporting electrolyte at a scan rate of 50 mV/s at 25°C. Standardized to Fc^+/Fc . a) reductive cycle b) oxidative cycle 64
- Figure 2.15** Cyclic voltammogram of compound 5 in dry acetonitrile and 0.1 M tetrabutyl ammonium perchlorate as supporting electrolyte at a scan rate of 50 mV/s at 25°C. Standardized to Fc^+/Fc 66
- Figure 3.1** Iridium pincer complexes. a) $(^tBu_4-POCOP)Ir$, b) $(^tPr_4-PCP)Ir$ and c) $(^tBu_4-PCP)Ir$, (adapted from reference) 76
- Figure 3.2** Schematic representation of the X-ray structures, a) top: $(CuCN)_3(Me_2S)$, bottom $(CuCN)(THT)$. (THT = tetrahydrothiophene), b) $(CuCN)L_n$ irradiated at 254 and 365nm; the polymers represented in a) are represented as 28b and 29 77
- Figure 3.3** Chalcogenide-based hexanuclear copper cluster: $[Cu_6L_2(O^tC(CH_3)_3)_2]$, where $L = C(Ph_2P=NSiMe_3)_2^{2-}$, (adapted from reference) 82
- Figure 3.4** Calculated crystal structure of $\{[(C_4H_8O)_4Li_3(CH(Ph_2P=N)_2)_2]^+ [CuCl_2]^- \}$, two complexes comprise the unit cell denoted as A (left complex) and B (right complex) 85
- Figure 3.5** Tri-lithium bis(iminodiphenylphosphorano)methanide 85

copper (I) dichloride

- Figure 3.6** *Tri-lithiated salts for battery applications. TLS-1, 86*
[N-lithium bis(carboxylithium methanesulfon)imide];
TLS-2, [N-lithium bis(4-lithiumsulfonatobutane)sulfonimide];
TLS-3, [N-lithium bis(o-
lithiumsulfonatoacetophenonyl)sulfonimide]
- Figure 3.7** *ORTEP of 88*
[(CH₃)₃CCH₂]₂[CH₂C(CH₃)₂CH₂]-Cr[Li(TMEDA)]₂.
Thermal ellipsoids were drawn at 50% the probability
level

List of Schemes

Scheme 1.1	<i>General binding attacks for the formation of a pincer complex</i>	6
Scheme 1.2	<i>NCN palladium-based pincer catalyst capable of multiple carbon-carbon bond formations (adapted from reference)</i>	12
Scheme 1.3	<i>CNC pincer complex used in water catalyzed Suzuki reaction</i>	14
Scheme 1.4	<i>Condensation reaction of N-sulfonylimines and methyl isocyanoacetate, catalysed by a chiral palladium-based pincer complex (figure adapted from reference)</i>	16
Scheme 1.5	<i>Staudinger reaction mechanism</i>	17
Scheme 1.6	<i>Formation of bis(diphenyltrimethylsilyliminophosphorano)methane</i>	17
Scheme 1.7	<i>Synthesis of phosphorus-stabilized lanthanide carbenes</i>	20
Scheme 1.8	<i>Proposed pathways for the Ullmann reaction</i>	23
Scheme 1.9	<i>N-arylation of pyrazole with 4-iodoacetophenone using a copper catalyst (scheme adapted from reference)</i>	25
Scheme 2.1	<i>Deprotonation of bis(diphenyltrimethylsilyliminophosphorano)methane to bis(diphenyltrimethylsilyliminophosphorano)methanediide</i>	35
Scheme 2.2	<i>Reaction pathways for the formation of pincer chelates</i>	39
Scheme 2.3	<i>Reaction of 2 with a chromium precursor to form $[Cr_2(\mu-Cl)_2\{\mu_2-C(Ph_2P=NSiMe_3)_2-\kappa^4C,C',N,N'\}(LiCl)(THF)_2\}_2$ and subsequent rearrangement to a stable form $[Cr\{\mu_2-C(Ph_2P=NSiMe_3)_2-\kappa^4C,C',N,N'\}]_2$</i>	42
Scheme 2.4	<i>Adapted pincer scheme for the reaction of Li_2L and $[Cu_2Cl_2(cod)_2]$ (top), actual hexanuclear copper cluster scheme (bottom)</i>	51
Scheme 3.1	<i>Capping ligand, X, exchanged with a chalcogenide-based precursor, Y, to form a new cluster with Y at the caps</i>	78

Scheme 4.1 *Proposed reactions using
bis(diphenylthiophosphinoyl)methaniide*

List of Symbols, Nomenclature, and Abbreviations

Å	angstrom
λ	wavelength
°C	degrees Celsius
eV	electron volt
EtOH	ethanol
MeOH	methanol
mL	millilitre
H ₂ O	water
H ₂ L	CH ₂ (Ph ₂ PNSiMe ₃) ₂
Li ₂ L	[CLi ₂ (Ph ₂ PNSiMe ₃) ₂] ₂
L	[C(Ph ₂ PNSiMe ₃) ₂] ⁻²
PL	photoluminescence
V	volt
ppm	parts per million
UV	ultraviolet
UV-vis	ultraviolet-visible
mol	mole
m	milli (10 ⁻³)
RBF	round bottom flask
THF	tetrahydrofuran
cod	cyclooctadiene
MLCT	metal-to-ligand charge transfer
LMCT	ligand-to-metal charge transfer
XMCT	halide-to-metal charge transfer
NMR	nuclear magnetic resonance
MS	mass spectroscopy
TGA	thermal gravimetric analysis
EA	elemental analysis
E.S.U.	electrostatic unit
Hz	Hertz

Chapter 1:

From Carbon, to Complexes,

To Catalysis and

Onwards to Copper

1.1 Carbon, the Element

Carbon is a central element in the periodic table. Through the use of four valence electrons, carbon can form up to four stable bonds. Through 4 sp^3 hybridized orbitals carbon can achieve an optimal stability, whilst retaining reactivity towards other biological and chemical influences.^{1,2} Carbon often forms the base for which many multifarious compounds are derived using carbon in a coordinating ligand.

Making a divalent carbon species, where only two of the electrons on carbon are involved in bonding to substituents, R_2C^{-2} , was, initially, thought to form briefly through a transition state. Scientists have since discovered many divalent carbon species, including the carbene.³

In 1931, Sidgwick reported the unique bonding motif for carbon in compounds such as carbon monoxide and isocyanides.³ These compounds showed bonding never before understood. Unlike a ketone or an aldehyde, in which a dipole is very clearly outlined, this class of compounds showed a cooperative bonding. For example, in carbon monoxide, the oxygen possesses a dipole of 5.4 (dipoles are measured with units of 10^{-18} E.S.U.) towards carbon whilst carbon has a dipole of 5.3 towards oxygen, which results in an overall dipole towards carbon of 0.12. The identification of this dipole moment directed toward carbon was a breakthrough in the understanding the bonding characteristics of carbon species including carbene-containing compounds.

Carbenes were initially classified as either Fischer carbenes or Schrock carbenes, later additional subsets of carbenes were introduced. Herein, the

discussion will focus on three types of carbenes (i.e., Fischer, Schrock and the geminal dianion) illustrated in Figure 1.1.^{4,5}

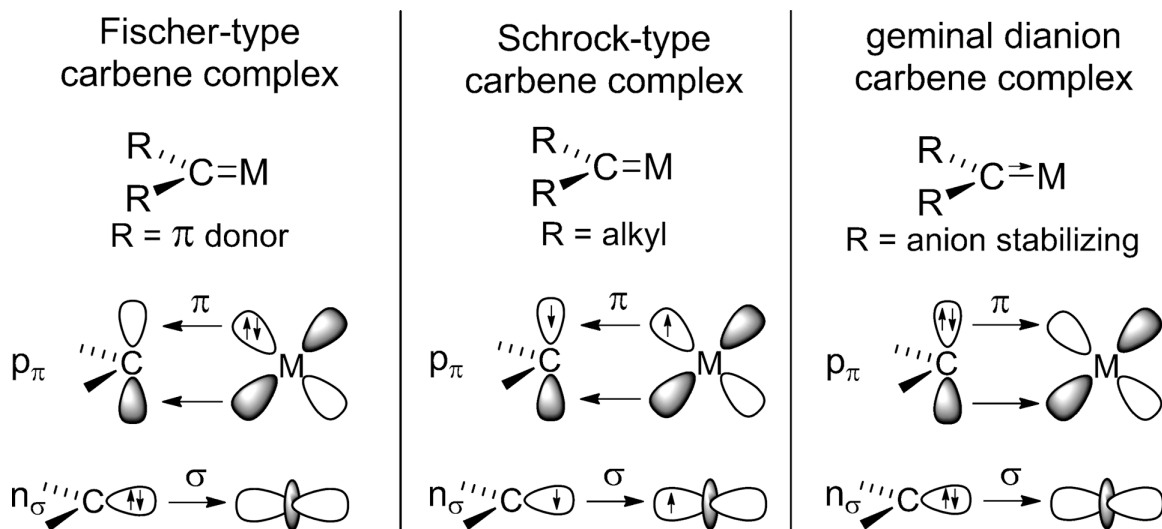


Figure 1.1: Types of metal carbene species⁶

1.2 Fischer, Schrock and Geminal Dianions

Carbon double bonds commonly refer to carbenes, whether they are carbon-nitrogen double bonds or carbon-metal double bonds or another variation of the sort. The basis of a carbene is a di-substituted carbon, $RR'C:$ with a lone pair available for donation. They are unlike olefins in that the olefin bond is formed from equal contribution of electron density from each supporting atom. For carbenes donation is predominately into an adjoining species, $RR'C \rightarrow M$. It should be noted that back-donation can occur to afford additional stability of the carbene species.

1.2.1 Fischer Carbenes

Fischer-type carbenes consist of C on the metal and π -back-donation from a filled d-orbital into an empty p-orbital on the carbon atom. Fischer carbenes (Figure 1.1) have a large energy gap between the singlet and triplet state as a result of the bonding configuration and electron donation.⁷⁻⁹ The elongated double bond formed is related closer to that of a single bond through the formation of a σ -bond first, then the back-donation, thereby making the carbene a good electrophile.^{10,11}

1.2.2 Schrock Carbenes

Schrock carbenes (e.g. alkylidenes) are formed through the interaction between alkyl substituents and the metal centre to form a covalent carbon-metal bond. Bond formation in Schrock carbenes consists of σ -donation into a half-filled orbital on the metal and similar donation of a π -electron from the metal's d-orbital to a half-filled p-orbital. These carbenes are generally nucleophilic and have an interactive and sharing approach with regard to electrons between the carbon and metal.^{5,12,13}

1.2.3 Geminal Carbenes

A geminal dianion carbene complex can be formed through the deprotonation, or dilithiation, of an alkyl backbone forcing the carbon to become a reactive carbene due to the high electron density on the carbon atom. The formation of the carbon-metal bond, represented in Figure 1.1, is through a four-

electron donation into the metal centre, two electrons through σ -donation and two electrons through π -donation. The nucleophilic carbon is stabilized through the use of anion stabilizing groups, typically using groups that are bulky. Silyl groups are often chosen for this purpose as they are highly polarizable and the groups have σ^* -SiR orbitals that are relatively lower in energy allowing for negative hyperconjugation with the carbon atom. Negative hyperconjugation can be viewed as a donation of electron density from filled π -orbitals to the available σ^* -orbitals on the silyl groups assisting in the stabilization of the highly reactive carbene species formed.⁶

This thesis will focus on the application of carbenes in pincer ligands.

1.3 Origin of the Term Pincer

The term “pincer” draws its roots from the military maneuver in which a military force completely encircles their enemy on both flanks and front, thereby cutting off any outward motion, as well as forward motion of the incoming army. The first and arguably the most successful execution of this double flank type attack was recorded in 216 BC at the Battle at Cannae, the final battle in the second Punic war. Hannibal over took the Roman opposition by using his Carthaginian army as the frontal attacking force and the assisting African infantry as the flanking attackers, engulfing the Roman army, and forcing one of the most bloody battles ever recorded.¹⁴

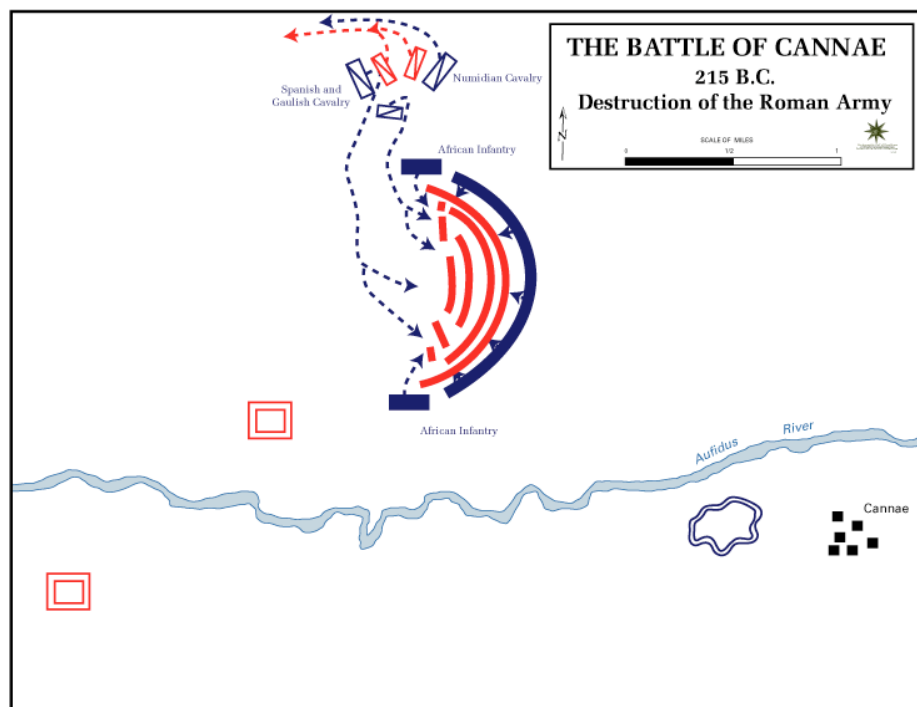
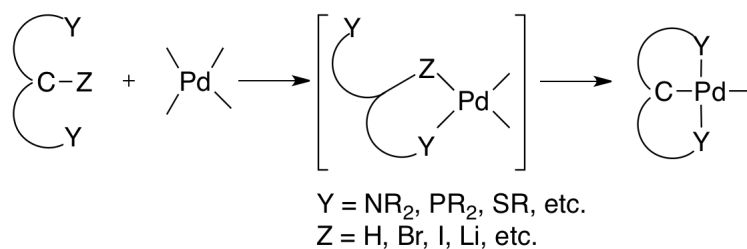


Figure 1.2: Battle of Cannae during the Second Punic war depicting the pincer maneuver attack tactic¹⁵

1.3.1 Pincers: From the Battlefield to the Laboratory

The general pincer ligand-metal structure, Scheme 1.1, can be structurally compared to the battle technique. The metal, in this case, Pd, would be the Roman army. The central binding site, C, would be the Carthaginian army while the remaining two binding sites, Y, would represent the assisting African infantry.¹⁶



Scheme 1.1: General binding attacks for the formation of a pincer complex¹⁶

The common notation for the description of a pincer complex involves denoting the atoms directly bonded to the metal centre. The format is: a flanking atom, the main centre binding atom and finally the second flanking atom; referring back to Scheme 1.1 the notation would be YCY. For example, a PCP ligand would be bonded to the metal centre via a central carbon atom, that typically is located down the midway of a ligand and the two phosphorus atoms flank the metal centre adding stability. A specific example, the NCN structural motif, of this type of ligand is shown later, in Figure 1.5. A general NCN ligand possesses two nitrogen-based metal bonding sites flanking the metal centre and a third C-based bonding centre. This tridentate ligand structure affords increased stability of the metal to ligand structure while still maintaining an active level of catalytic activity at the metal centre. In addition, the structure of the backbone is exquisitely tailorable and allows for introduction of varying degrees of steric bulk, that can influence reactivity at the metal centre.^{17,18}

1.4 Ligand Design

The composition of a ligand may be tailored depending upon its intended use. It is designed to address many issues including balancing stability and reactivity with the push and pull of electrons toward the active species. Ligands are not simply chosen based upon ease of synthesis; they play an intrinsic role in overall formation and consequent reactivity of a compound. Ligands function in a manner similar to that of a directing or functional group, wherein the ligand is

composed of atoms that have electron donating or withdrawing qualities that are desirable to the molecule based on their proximity to the carbene moiety.

1.4.1 Steric Effects on Ligand Design

Steric hindrance, created through the use of bulky ligands can limit or even prevent reactivity at a specific site. Ligands used to increase bulk around a carbene centre are often bonded to heteroatoms adjacent to the carbene species, thus changing the electronics according to complex design and necessity.

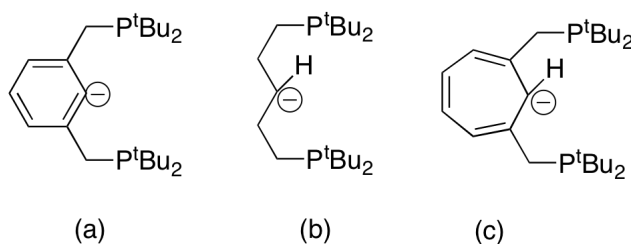


Figure 1.3: PCP-pincer backbone ligands: (a) aryl, (b) alkyl and (c) cycloheptatrienyl ligand¹⁹

In a review of three types of pincer ligands: alkyl, aryl and cycloheptatrienyl, the ligands were compared with regard to flexibility, stability and reactivity.¹⁹ All three ligand types form five-membered rings with the metal atom that are thermodynamically stable; however, each ligand forces different degrees of stabilities through: bite angles, electronics and sterics of the binding atoms to the metal, and orbital overlap. Alkane-based ligands (see Figure 1.3 (b)) encourage high flexibility in the molecule and also boast high electron donating abilities through the sp^3 *ipso*-carbon bound to the metal centre. However, these types of ligands are also subject to olefin isomerization when given the

opportunity, through hydrides in a trans configuration, undergoes a hydride shift (see Figure 1.4). The olefin isomer is more stable than the carbene isomer by 2.9 kcal/mol; therefore, β -H atoms need to be avoided. Alkane ligands as backbones are known for their high reactivity.

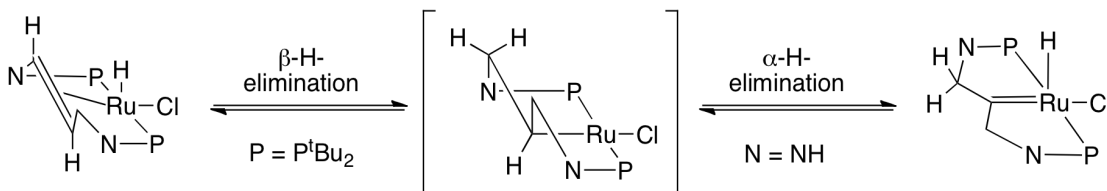


Figure 1.4: Equilibrium between carbene and olefin complexes, achieved through α -H- and β -H-elimination, respectively¹⁹

Backbones containing an aryl group directly bonded to the metal (see Figure 1.3 (a)) can handle various chemical intermediates through the delocalization of π -electrons about the ring system, which can be advantageous or detrimental. Functional groups in the para-position of the aryl can be electron donating or be electron withdrawing thereby pushing or pulling electron density around the metal centre, which may aid in stabilizing the complex through subsequent reaction mechanisms. The use of aryl groups as ligand backbones is popular due to the inherent stability and ease of reactivity control compared to alkane backbone ligands. In an effort to balance reactivity and stability ligand backbones are tailored to meet the desired requirements.^{20,21}

Cycloheptatrienyl ligands (see Figure 1.3 (c)) have the advantage of being capable of binding in three different motifs; η^1 -carbene, η^2 -allene and η^7 -tropylium. The metal dictates the preferred bonding mode: early transition metals

prefer the carbene configuration because of the tropylium resonance form (i.e., aromatic tropylium cation) and ensued aromaticity; however, late transition metals vary based on their electron density. For example, Pd⁰ favours allene formation, while lower density, e.g. Pd^{II}, metals prefer a carbene format. The cycloheptatrienyl ligand offers the stability of an aryl ligand with the reactivity of an alkane ligand.

While the discussion above has primarily focused on the center of the three points of attachment to a metal center, the flanking coordinating atoms are important factors and must be chosen with some care and consideration.

1.4.2 Nitrogen Versus Phosphorus

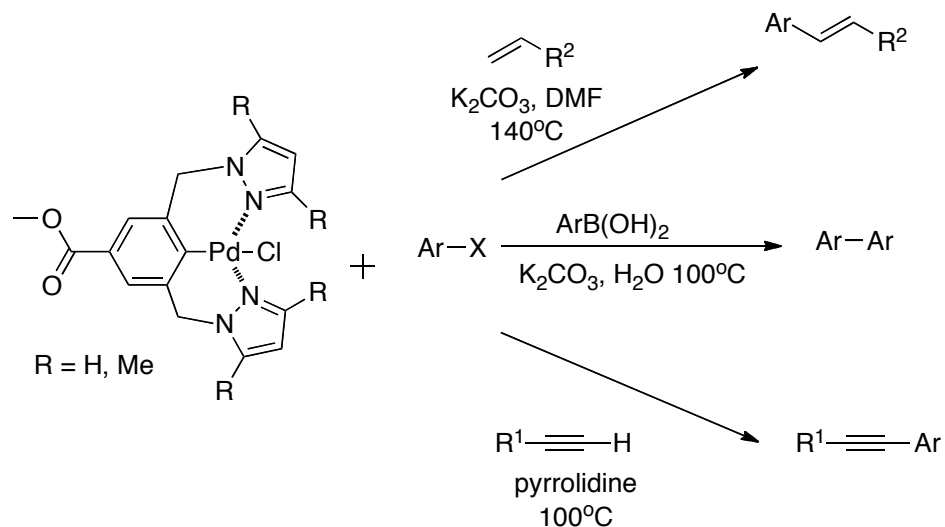
Typical candidates are phosphorus and nitrogen given their lone pairs of electrons, which are available for coordination with metal centres. The electrons are used to stabilize the carbene through π -donation into the empty p $_{\pi}$ -orbitals on the carbene. Nitrogen is the better donor as the reduced energy demand to achieve a planar environment for easier donation can be better attained by nitrogen than by phosphorus, which allows for easier s-p hybridization. Phosphorus also has an inherent reluctance to s-p hybridize due to the larger size in general despite the fact that an overall stability increase in the structure would be attained. The benefits of using phosphorus atoms may be gained in the electronic properties and reactivity of the carbene. Through the reduction in highly reactive carbene character perturbation towards metal precursors to form stable yet seemingly reactive compounds.²²

1.5 Pincers and Catalysis

Carbon-carbon bonds are critical structural motifs within functional materials such as polymers, olefin polymerization and pharmaceutical applications, synthesis of new drugs through the use of cross-coupling reactions to increase the frequency of convergent syntheses over the less favourable linear synthetic routes.²³⁻³² Pincer catalysts can also be chiral.³³ For this reason, establishing procedures for their formation is of great fundamental and practical interest. Current research in this regard has included the design, synthesis, and application of countless catalysts.

1.5.1 The Big Catalysis Players: Heck, Sonogashira and Suzuki

Certain cross-coupling reactions are so well known they barely need an introduction. The Heck, Sonogashira and Suzuki reactions are but a few examples of carbon-carbon bond-forming reactions that shaped chemistry. They have sparked a quest for faster, more efficient coupling catalysts (Scheme 1.2).³⁴⁻⁴³



Scheme 1.2: NCN palladium-based pincer catalyst capable of multiple carbon-carbon bond formations (adapted from reference)¹⁷

The NCN pincer complex, Figure 1.5 (a), was shown to have adequate catalytic reactivity in the Heck and Sonogashira reaction and excellent reactivity in regards to the Suzuki reaction, with turn over numbers (TON) ranging from 71 000 to 8 600 000 coupled with high yields. PCP complexes (i.e. Figure 1.5 (b)) have been widely studied and perform nicely under a variety of conditions and for many types of catalytic cycles and reactions, including cross-coupling and α -arylation of ketones.¹⁷

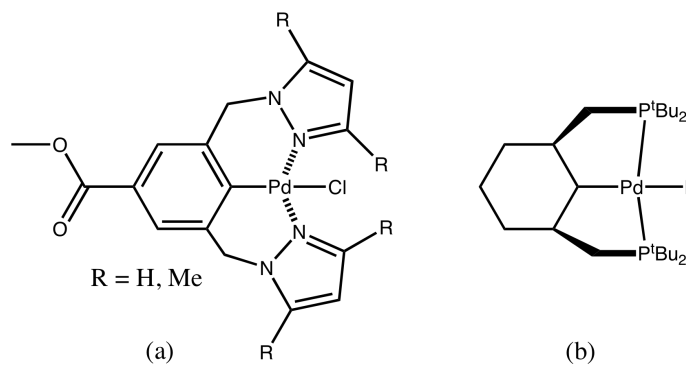


Figure 1.5: (a) NCN pincer complex (b) PCP pincer complex, with palladium metal centres, used as catalysts for Heck, Sonogashira and Suzuki reactions¹⁷

An example of pincer complexes being used as catalysts for the Suzuki reaction, shown by Moreno *et al.*, focused extensively on creating a compound with high catalytic activity, ease of separation and reusability.¹⁷ Banking on the previous modest success of CNC pincer compounds that were anchored to structures such as clays and solid polymers they sought to design a compound that could be easily separated. Through the use of an organic solvent the desired product could be isolated, with the newly formed C-C bonds, leaving behind the catalyst in aqueous media for further use with additional reagents in subsequent reactions.

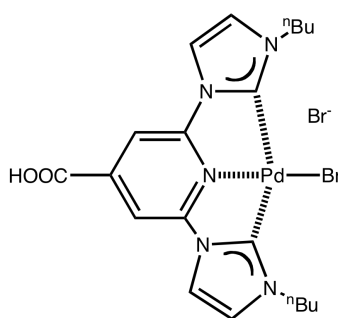
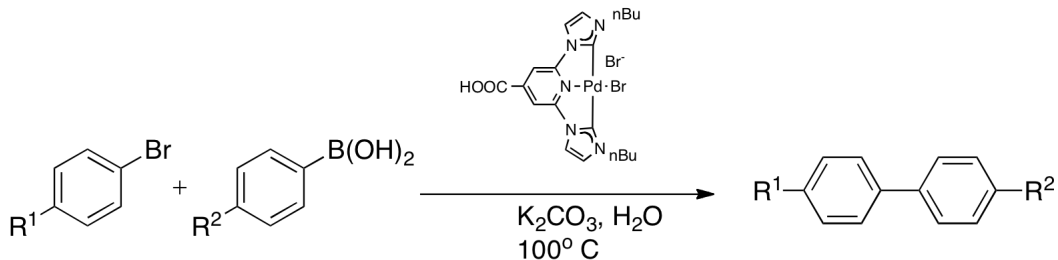


Figure 1.6: CNC reusable pincer for Suzuki reactions¹⁷

The CNC pincer shown in Figure 1.6, displayed all of the desired qualities: extremely high catalytic activity, with TON reaching as high as 10^9 , easily isolable products through a diethyl ether extraction and a reusability rate of up to 5 repetitions prior to the catalyst shutting down. The most successful catalysis reaction can be seen below in Scheme 1.3.



Scheme 1.3: CNC pincer complex used in water catalyzed Suzuki reaction¹⁷

1.5.2 Unsymmetric Pincer Ligands

Unsymmetric pincer ligands are compounds in which the flanking atoms are not the same. They are thought to exhibit unique accessibility in reactivity due to the presence of two different donor groups. Some examples of unsymmetrical pincer compounds can be seen in Figure 1.7. The palladacycle compounds, (a) and (b), are examples of PCN compounds that have shown promising results in the area of C-C cross-coupling with regard to aryl halides and aryl boronic acids.^{17,44,45}

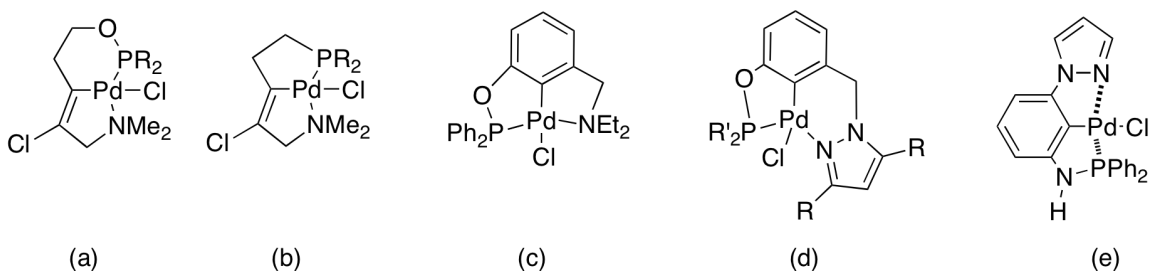


Figure 1.7: Unsymmetrical PCN pincers used for various cross-coupling reactions¹⁷

The unsymmetrical pincer (e) has shown a useful presence as the first unsymmetrical catalyst used for Suzuki couplings, Sonogashira and Hiyama,

wherein yields ranged from 35-99% upon using catalyst quantities between 0.1-4% mol. Although unsymmetrical pincer compounds have shown promise as catalysts, the field of study is not nearly as extensive as that of symmetrical compounds.

1.5.3 Asymmetric Pincer Ligands

Achiral pincer complexes, for the use in asymmetrical catalysis reactions, have recently become a thriving field of study as well. Allylation of sulfonimines, aldol, silylcyanation and condensation reactions are a few of the reactions where the usage of chiral catalysts are applicable.⁴⁶⁻⁴⁸ Chiral pincer catalysts (Figure 1.8) have been used in asymmetric catalysis for the high yielding condensation reactions of sulfonimines and isocyanacetate with good enantioselectivity, 86% ee, see below for an example (Scheme 1.4). The reaction produces both anti and syn forms; the use of a chiral catalyst pushes the favourability of one enantiomer preferentially, in this case the (2*S*,3*S*)-syn.

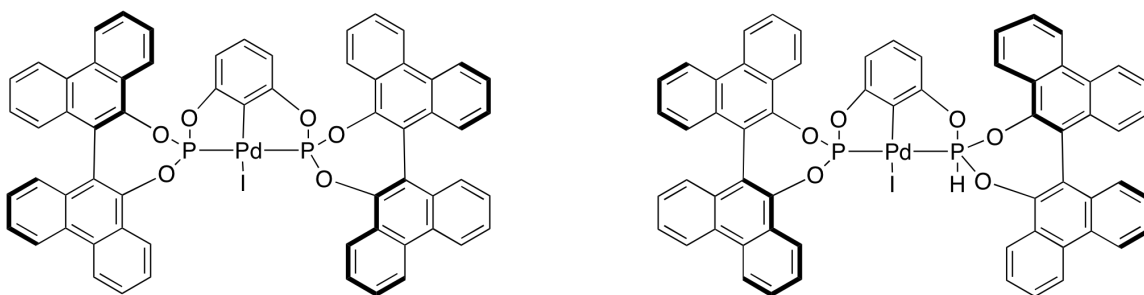
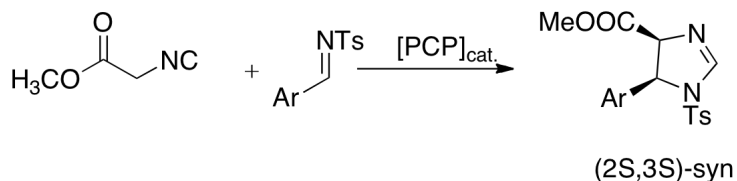


Figure 1.8: Palladium-based chiral pincer catalysts for condensation reactions⁴⁸

Each catalyst has a slight variation in ligand design and metal bonding environment, which in part translates into unique reactivity under similar conditions.



Scheme 1.4: Condensation reaction of *N*-sulfonylimines and methyl isocyanoacetate, catalysed by a chiral palladium-based pincer complex (figure adapted from reference)⁴⁸

1.6 Bis(diphenyltrimethylsilyliminophosphorano)methane

The ligand of choice for the research presented in this thesis begins with the molecule bis(diphenyltrimethylsilyliminophosphorano)methane, (**1**).⁴⁹

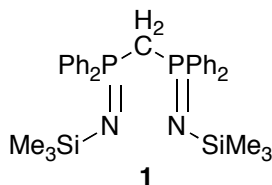
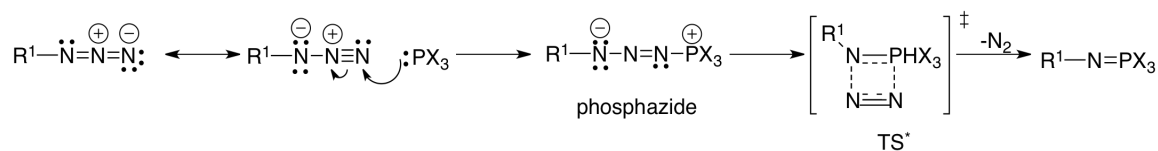


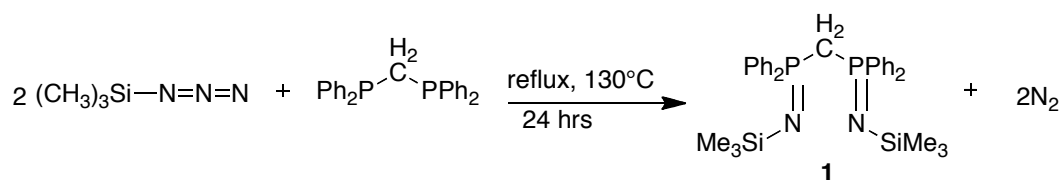
Figure 1.9: Bis(diphenyltrimethylsilyliminophosphorano)methane

First prepared in 1974 by Appel and Ruppert, its synthesis employs the Staudinger reaction: a one-pot, neat reaction between an azide and a tri-substituted phosphine to give an aza-ylide in quantitative yields. The mechanism of the Staudinger reaction is shown in Scheme 1.5.



Scheme 1.5: Staudinger reaction mechanism⁵⁰

The Staudinger reaction proceeds via nucleophilic attack of the phosphorus atom of the tri-substituted phosphine at the trimethylsilylazide centre to form a phosphazide. The phosphazide is then forced into a box shaped four-membered transition state, N₂ then dissociates releasing the iminophosphorane. The first step in ligand preparation involves nucleophilic attack causing oxidation of the bis(diphenylphosphino)methane compound. Following oxidation, two equivalents of trimethylsilylazide are added to the available reaction sites forming the desired **1** ligand and nitrogen gas (See Scheme 1.6).⁵¹



Scheme 1.6: Formation of bis(diphenyltrimethylsilyliminophosphorano)methane

1.6.1 Reactions of Compound 1

The chemistry of the compound **1** ligand has been explored extensively by *Cavell* and others have followed suit.⁵²⁻⁵⁶ Shown below are a few examples of transition and alkali metals complexes formed with **1**. In Figure 1.10, a four-coordinated nickel complex was formed using **1** and NiCl₂. The use of different

nickel salts yielded slight variations in the coordination of the ligand around the metal centre. The main feature to note is the six-membered ring system incorporating the metal and central pieces of the **1** backbone. It is also worth mentioning the benefits of phosphorus in the backbone. Classically, pincers backbones are written as, in the case of **1**, NCN; however a more applicable way of denoting the pincer backbone would be as a N(P)C(P)N, in order to exemplify the phosphorus atoms as being an essential part of the backbone. The phosphorus (V) atoms act similar to that of carbon in the bonding motifs, with additional flexibility to that of carbon enabling rigidity or flexibility in the backbone as necessary. As well, they become useful NMR markers, through ^{31}P NMR spectroscopy, allowing for reactions to be followed in situ.

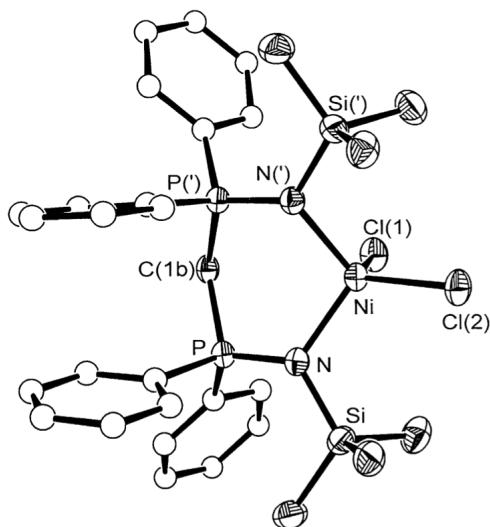


Figure 1.10: ORTEP representation of $\text{NiCl}_2[\text{CH}_2(\text{PPh}_2=\text{NSiMe}_3)_2]$. Thermal ellipsoids drawn at the 50% probability level (carbon atoms of phenyl rings are of arbitrary radius)⁵²

Similar to the work presented above was the work by Cavell *et al.*, wherein most of the recent research centered on the usage of **1** with various

precursors (Figure 1.11). Below are two examples of compounds, a zirconium and lithium, representing different binding techniques. The first, zirconium complex, depicts the pincer format of binding. The metal carbon bond separates the two fused five-membered rings and the metal centre is additionally stabilized by two toluene moieties. The second example takes **1** and deprotonates a single hydrogen species from the central carbon in the backbone forming the monoanion, which then reacts with the alkali metal precursor. The result is similar to that of the nickel complex; however, carbon-lithium interactions form a tridentate lithium, that almost resembles a pincer, which consequently forms two four-membered rings.

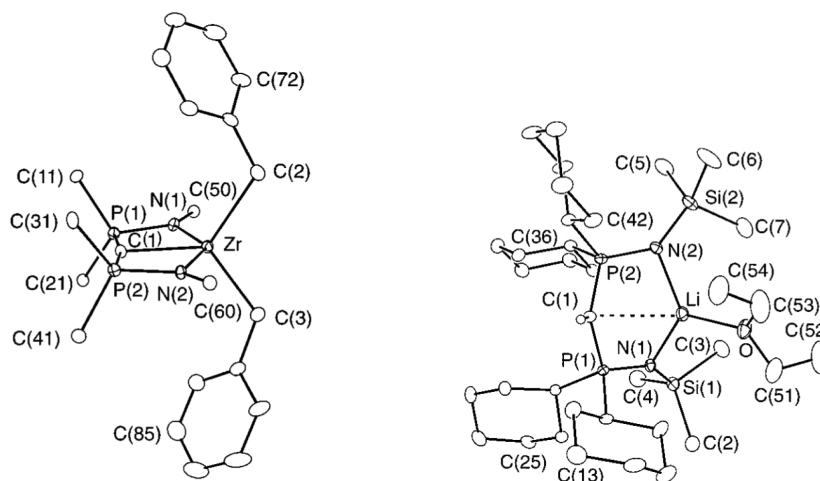
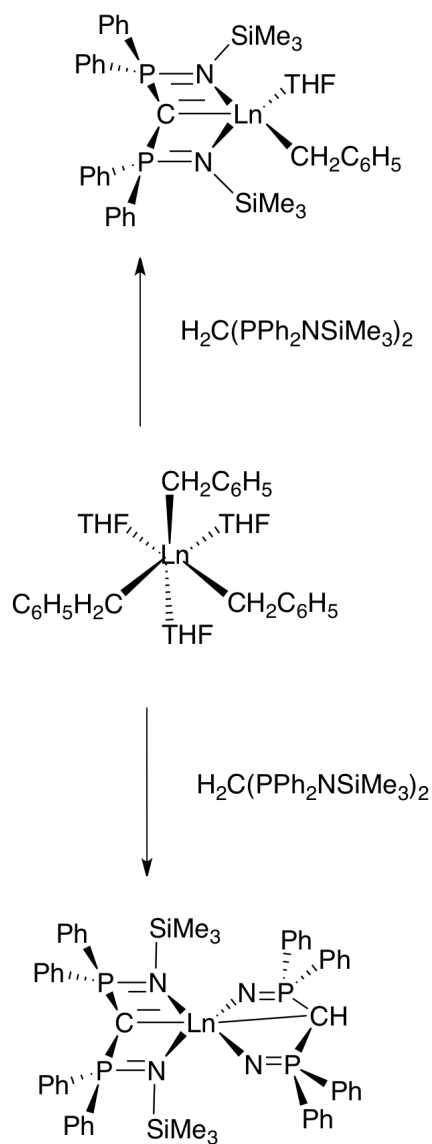


Figure 1.11: Left: ORTEP image of $[\text{Zr}\{\text{C}(\text{Ph}_2\text{P}=\text{NAd})_2-\kappa^3\text{C},\kappa\text{N},\kappa\text{N}'\}(\text{CH}_2\text{Ph})_2]$ Right: ORTEP image of $[\text{Li}\{\text{HC}(\text{Cy}_2\text{P}=\text{NSiMe}_3)_2-\kappa\text{C},\kappa\text{N},\kappa\text{N}'\}(\text{OEt})_2]$, atoms are represented by Gaussian ellipsoids at the 20% probability level^{54,55}

1.6.2 Recent Reactions of Compound **1**

Of late, Liddle *et al.* prepared numerous compound **1** complexes of lanthanide metals in an attempt to establish the bonding patterns between lanthanides and carbon species. Bond lengths, from X-ray crystallographic data,

were used to determine whether lanthanide compounds form alkyl bonds or alkylidene-type bonds. These protonated ligand complexes were subsequently used to prepare related pincer ligand complexes (See Scheme 1.7).^{23,57,58}



Scheme 1.7: Synthesis of phosphorus-stabilized lanthanide carbenes⁵⁷

Detailed investigation of the reaction mechanism afforded the process by which the two reagents come together to form a mono-protonated methanide compound, then an intramolecular deprotonation occurs allowing the complex to bind to a second mono-protonated chelating methanide ligand. The Liddle group has also demonstrated metal precursors (e.g., $Y(CH_2SiMe_3)_3(THF)$), which can deprotonate **1** selectively. Under these conditions, **1** is deprotonated and a rigid carbene containing complex is formed.^{59,60} The rigidity of the complex arises from the high structure bonding confirmation of the ligand as it binds to the metal centre in a carbene fashion. The double bond character between the carbon and, in this case, the yttrium atom, locks the metal centre in place and reduces flexibility at the previously freely rotating sp^3 carbon.

While many examples of **1** resulted in compounds containing methane or methanide moieties examples of methanide complexes derived from the protonated ligand also have appeared. Therefore, the chemistry was directed toward reactions with various metal precursors with the intentionally deprotonated ligand; in particular, the dilithiated bis(diphenyltrimethylsilyliminophosphorano)methanediide will be discussed in Chapter 2.

1.7 Copper as a Catalyst

The Ullmann reaction involves the reaction of two different aryl-halides, or two equivalents of the same aryl-halide, with one equivalent of a copper source at high reaction temperatures. This reaction yields the coupled biaryl product and

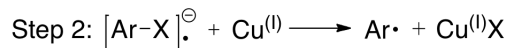
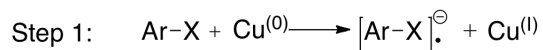
two equivalents of copper halide. When substituents (i.e., electron-withdrawing and donating groups) are placed in the ortho position of the aryl ring the reactivity of the aryl system increases.⁵⁰ Large bulky substituents placed ortho to the halide decrease the reactivity, as the steric bulk inhibits close access to the reaction sites. Typically, activated copper is used at high temperatures, above 200 °C. Sonication also improves reactivity. The Ullmann reaction has used copper (I) salts to form cross-coupled products.⁶¹ Originally, copper catalysts for the Ullmann reaction, were used in near stoichiometric amounts, which is not favourable due to the need for large amounts of catalyst. The ideal catalyst requires small amounts, which should be easily accessed, made of materials abundant in nature and relatively inexpensive. Palladium and platinum are the most common catalyst choices and are generally chosen over copper for their high efficiency; however, they are not nearly as abundant nor are they inexpensive.⁶²⁻⁶⁴

1.7.1 Cross-Coupling Reactions: Further Investigation on the Ullmann Reaction

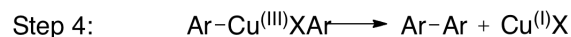
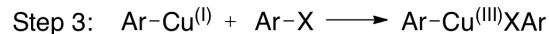
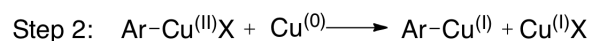
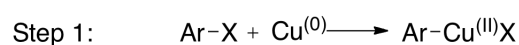
Cross-coupling reactions are generally classified as nucleophilic substitution reactions in which a nucleophile attacks an electrophile to form a new compound through the formation of a σ -bond with the aid of a catalyst. The Ullmann reaction mechanism is unknown; however, two pathways have been postulated, see Scheme 1.8. The catalysts chosen, originally copper (0) in nature, were added into the reaction mixture, where an oxidative addition reaction was

initiated with the metal, acting as a nucleophile, forming a copper (II) species. The copper (II) complex could be reduced to a copper (I) complex with the aryl substituent through the aid of Cu (0), which is oxidized in the process. A transmetallation reaction occurs where the copper (I) complex reacts with an adjacent non-complexed aryl halide followed by a reductive elimination releasing the newly formed compound, either a symmetrical or unsymmetrical biaryl compound and the original copper (I) catalyst. Reactions were pushed forward through the formation of the original copper (I) compounds.

Aryl radical pathway:



Arylcopper intermediates pathway:



Scheme 1.8: Proposed pathways for the Ullmann reaction⁵⁰

1.7.2 Cross-Coupling Reactions: Beyond the Ullmann reaction

Copper compounds have an extensive history of catalytic uses beyond those described above. Reactions classed under the category of ‘click chemistry’ include, 1,3-dipolar cycloaddition of alkynes and azides forming substituted triazoles.⁶⁵⁻⁷¹ Other reactions catalyzed by copper (I) include: the methanolysis of aryl bromides, to form methyl aryl ethers, can be achieved using CuBr and

sodium methoxide as co-catalysts, the formation of aryl-nitrogen bonds through the use of a $\text{Cu}(\text{PPh}_3)_3\text{Br}$ complex, as well as the hydrosilylation of ketones.⁷²⁻⁷⁴

1.7.3 Copper Catalysts: New Directions

Recently, the Biffis group formulated a trinuclear copper (I) complex, $[\text{Cu}_3(\text{BH}\{\text{N}(\text{H})\text{C}=\text{C}(\text{H})\text{N}(\text{Me})\text{C}\}_3)_2]^+$ with counter anion $[\text{BF}_4]^-$, that allowed the Ullmann reaction to proceed under milder conditions. The complex boasts two tricarbene ligands that bind sequentially to three copper atoms, wherein the copper atoms are bound to two imidazolin-2-ylidene rings, one from each of the carbene ligands, thereby the copper atoms act as bridges for the enveloping carbene ligands (Figure 1.12).

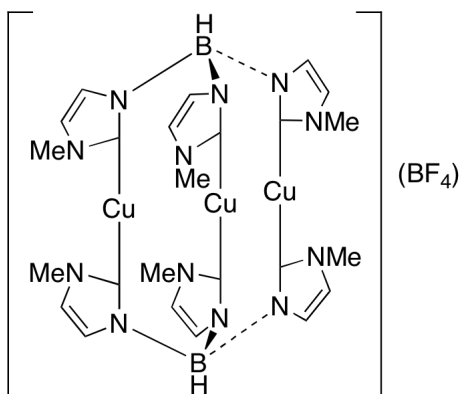
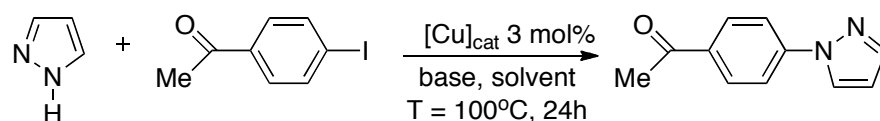


Figure 1.12: Bis[hydrotris(3-methyl-imidazolin-2-ylidene-1-yl)borate]tricopper(I) tetrafluoroborate⁷⁵

The most encouraging aspect of the chemistry involved the reduced temperature at which the reaction proceeded. The trinuclear complex has shown activity down to a reasonable 100 °C, within 24 hours whereas the previous copper catalysts required temperatures around and above 200 °C.⁷⁵ There was also

a reduction in the required amount of copper catalyst for the reaction to proceed. The trinuclear copper (I) complex was used in reactions in amounts ranging between 1-3% mol, even as low as 0.1% mol under extended reaction times, compared to 10% mol and upwards to a maximum of 100% mol required of catalytic copper in the original Ullmann reaction.⁷⁵ The reaction of focus for the trinuclear copper complex was the arylation of pyrazoles and other azoles as well as amides and phenols with various substituted aryl halides, bromine and iodine mainly, but some activated chlorides were also utilized (Scheme 1.9).



Scheme 1.9: N-arylation of pyrazole with 4-iodoacetophenone using a copper catalyst (scheme adapted from reference)⁷⁵

The formation of C-N bonds was thought to proceed in a similar fashion to the Ullmann reaction especially with regard to reaction conditions; however, the substitution on the aryl halide was shown to make no difference, unlike steric hindrances, which were consistent with the Ullmann reaction conditions and trends. Reaction turnovers were typically highly efficient as indicated by exceptional yields for many of the reaction trials. The amide arylations were not observed to be as successful as the azoles and phenols by comparison. Depression of the amide arylation reaction was suggested as the additional chelation of the amide to the copper complex thus deactivating the catalyst and rendering the reaction less efficient.

Copper (I), as illustrated above, can be used in a variety of ways. Through the following chapters the versatility of copper and compound **1** will be discussed to further research into the growing field of copper compounds.

1.8 Thesis Outline

The following chapters will detail research done within the Cavell lab over the course of two and a half years.

Chapter 2 will begin with a brief introduction to copper followed by a detailed discussion into one of the starting ligands, bis(diphenyltrimethylsilyliminophosphorano)methaniide. The formation of complexes with the ligand will then be introduced and the variations in bonding types described. The hexanuclear copper clusters will be the main focus of the chapter with an in depth discussion on their luminescence and electronic properties.

Chapter 3 will introduce the different exchange reactions attempted on the hexanuclear copper clusters and how the reactivity changed accordingly. This will be followed with an evaluation, what worked and what did not, and analysis into the formation of a tri-lithium cluster.

The thesis will close, in Chapter 4, with remarks on the direction wherein the research could be taken and some conclusions based on the results gathered over the course of this research.

1.9 References

- (1) Petrucci, R. H.; Harwood, W. S.; Herring, F. G. *General Chemistry: Principles and Modern Applications*; 8th ed.; Prentice Hall, **2002**, 1-1160.
- (2) Housecroft, C. E.; Sharpe, A. G. *Inorganic Chemistry 2nd edition*; Pearson Education Limited: Harlow, England, **2005**, 1-949.
- (3) Sidgwick, N. V. *Chemical Reviews* **1931**, 9, 77-88.
- (4) Coalter III, J. N.; Bollinger, J. C.; Huffman, J. C. *New J. Chem.* **2000**, 24, 9-26.
- (5) Occhipinti, G.; Jensen, V. R. *Organometallics* **2011**, 30, 3522-3529.
- (6) Gessner, V. H. *Organometallics* **2011**, 30, 4228-4231.
- (7) Nandi, B.; Sinha, S. *Tetrahedron* **2011**, 67, 106-113.
- (8) Barluenga, J.; Vicente, R.; López, L. A.; Tomás, M. *Journal of Organometallic Chemistry* **2006**, 691, 5642-5647.
- (9) Baldoli, C.; Cerea, P.; Falciola, L.; Giannini, C.; Licandro, E.; Maiorana, S.; Mussini, P.; Perdicchia, D. *Journal of Organometallic Chemistry* **2005**, 690, 5777-5787.
- (10) Dötz, K. H.; Stendel, J. *Chemical reviews* **2009**, 109, 3227-74.
- (11) Frémont, P. de; Marion, N.; Nolan, S. P. *Coordination Chemistry Reviews* **2009**, 253, 862-892.
- (12) Schrock, R. R. *Chemical reviews* **2009**, 109, 3211-26.
- (13) Schoeller, W. W.; Rozhenko, A. J. B.; Alijah, A. *Journal of Organometallic Chemistry* **2001**, 617-618, 435-443.
- (14) Daly, G. *Cannae: The Experience of Battle in the Second Punic War*; Taylor & Francis, **2002**.
- (15) Martini, F. The Department of History, United States Military Academy.
- (16) Morales-Morales, D. *The chemistry of pincer compounds*; Elsevier Science, **2007**, 3, 1-444.

- (17) Moreno, I.; SanMartin, R.; Inès, B.; Churruca, F.; Domínguez, E. *Inorganica Chimica Acta* **2010**, *363*, 1903-1911.
- (18) Nilsson, P.; Wendt, O. F. *Journal of Organometallic Chemistry* **2005**, *690*, 4197-4202.
- (19) Leis, W.; Mayer, H.; Kaska, W. *Coordination Chemistry Reviews* **2008**, *252*, 1787-1797.
- (20) Krogh-Jespersen, K.; Czerw, M.; Zhu, K.; Singh, B.; Kanzelberger, M.; Darji, N.; Achord, P. D.; Renkema, K. B.; Goldman, A. S. *Journal of the American Chemical Society* **2002**, *124*, 10797-809.
- (21) Riehl, J. F.; Jean, Y.; Eisenstein, O.; Pelissier, M. *Organometallics* **1992**, *11*, 729-737.
- (22) Vignolle, J.; Cattoën, X.; Bourissou, D. *Chemical reviews* **2009**, *109*, 3333-84.
- (23) Mills, D. P.; Soutar, L.; Lewis, W.; Blake, A. J.; Liddle, S. T. *Journal of the American Chemical Society* **2010**, *132*, 14379-14381.
- (24) So, C. M.; Kwong, F. Y. *Chemical Society reviews* **2011**, *40*, 4963-72.
- (25) Britovsek, G. J. P.; Gibson, V. C.; Wass, D. F. *Angewandte Chemie International Edition* **1999**, *38*, 428-447.
- (26) Brintzinger, H. H.; Fischer, D.; Mülhaupt, R.; Rieger, B.; Waymouth, R. M. *Angewandte Chemie International Edition in English* **1995**, *34*, 1143-1170.
- (27) Bochmann, M. *Journal of the Chemical Society, Dalton Transactions* **1996**, 255.
- (28) Kaminsky, W. *Journal of the Chemical Society, Dalton Transactions* **1998**, 1413-1418.
- (29) Li, H.; Yang, M.; Pu, Q. *Microporous and Mesoporous Materials* **2012**, *148*, 166-173.
- (30) Terao, J.; Kambe, N. *Accounts of Chemical Research* **2008**, *41*, 1545-54.
- (31) Martin, R.; Buchwald, S. L. *Accounts of Chemical Research* **2008**, *41*, 1461-73.
- (32) Würtz, S.; Glorius, F. *Accounts of Chemical Research* **2008**, *41*, 1523-33.

- (33) Wallner, O. A.; Olsson, V. J.; Eriksson, L.; Szabó, K. J. *Inorganica Chimica Acta* **2006**, *359*, 1767-1772.
- (34) Rosa, J. C. de la; Diaz, N.; Carretero, J. C. *Tetrahedron Letters* **2000**, *41*, 4107-4111.
- (35) Rosol, M.; Moyano, A. *Journal of Organometallic Chemistry* **2005**, *690*, 2291-2296.
- (36) Bagherzadeh, M.; Amini, M.; Ellern, A.; Keith Woo, L. *Inorganica Chimica Acta* **2011**.
- (37) Li, P.; Wang, L.; Li, H. *Tetrahedron* **2005**, *61*, 8633-8640.
- (38) Ye, Z.-W.; Yi, W.-B. *Journal of Fluorine Chemistry* **2008**, *129*, 1124-1128.
- (39) Bakherad, M.; Keivanloo, A.; Bahramian, B.; Hashemi, M. *Tetrahedron Letters* **2009**, *50*, 1557-1559.
- (40) Masuyama, Y.; Sugioka, Y.; Chonan, S.; Suzuki, N.; Fujita, M.; Hara, K.; Fukuoka, A. *Journal of Molecular Catalysis A: Chemical* **2011**, *352*, 81-85.
- (41) Hosoya, T.; Inoue, A.; Hiramatsu, T.; Aoyama, H.; Ikemoto, T.; Suzuki, M. *Bioorganic & medicinal chemistry* **2009**, *17*, 2490-6.
- (42) Joshaghani, M.; Faramarzi, E.; Rafiee, E.; Daryanavard, M.; Xiao, J.; Baillie, C. *Journal of Molecular Catalysis A: Chemical* **2006**, *259*, 35-40.
- (43) Durap, F.; Rakap, M.; Aydemir, M.; Özkar, S. *Applied Catalysis A: General* **2010**, *382*, 339-344.
- (44) Gong, J.-F.; Zhang, Y.-H.; Song, M.-P.; Xu, C. *Organometallics* **2007**, *26*, 6487-6492.
- (45) Rosa, G.; Rosa, C.; Rominger, F.; Dupont, J.; Monteiro, a *Inorganica Chimica Acta* **2006**, *359*, 1947-1954.
- (46) Wallner, O. a.; Olsson, V. J.; Eriksson, L.; Szabó, K. J. *Inorganica Chimica Acta* **2006**, *359*, 1767-1772.
- (47) Yoon, M. S.; Ramesh, R.; Kim, J.; Ryu, D.; Ahn, K. H. *Journal of Organometallic Chemistry* **2006**, *691*, 5927-5934.
- (48) Aydin, J.; Rydén, A.; Szabó, K. J. *Tetrahedron: Asymmetry* **2008**, *19*, 1867-1870.

- (49) Appel, R.; Ruppert, I. *Zeitschrift Fur Anorganische Und Allgemeine Chemie* **1974**, *406*, 131-144.
- (50) Kürti, L.; Czako, B. Hayhurst, J., Ed.; Elsevier Inc. **2005**, 1-758.
- (51) Staudinger, H.; Meyer, J.; Phosphinimine, P. *Helvetica Chimica Acta* **1919**, *2*, 635-646.
- (52) Ganesan, M. *Inorganica Chimica Acta* **2003**, *346*, 181-186.
- (53) Panda, T. K.; Roesky, P. W. *Chemical Society Reviews* **2009**, *38*, 2782-2804.
- (54) Kamalesh Babu, R. P.; McDonald, R.; Decker, S. A.; Klobukowski, M.; Cavell, R. G. *Organometallics* **1999**, *18*, 4226-4229.
- (55) Kamalesh Babu, R. P.; Aparna, K.; McDonald, R.; Cavell, R. G. *Organometallics* **2001**, *20*, 1451-1455.
- (56) Cavell, R. G. In *The Chemistry of Pincer Compounds*; Elsevier Science B.V. **2007**, 311-346.
- (57) Wooles, A. J.; Mills, D. P.; Lewis, W.; Blake, A. J.; Liddle, S. T. *Dalton Transactions* **2010**, 500-10.
- (58) Wooles, A. J.; Cooper, O. J.; McMaster, J.; Lewis, W.; Blake, A. J.; Liddle, S. T. *Organometallics* **2010**, *29*, 2315-2321.
- (59) Mills, D. P.; Wooles, A. J.; McMaster, J.; Lewis, W.; Blake, A. J.; Liddle, S. T. *Organometallics* **2009**, *28*, 6771-6776.
- (60) Liddle, S. T.; McMaster, J.; Green, J. C.; Arnold, P. L. *Chemical Communications* **2008**, *78*, 1747-9.
- (61) Beletskaya, I. P.; Cheprakov, A. V. *Coordination Chemistry Reviews* **2004**, *248*, 2337-2364.
- (62) Sperotto, E.; Vries, J. G. de; Klink, G. P. M. van; Koten, G. van *Tetrahedron Letters* **2007**, *48*, 7366-7370.
- (63) Sperotto, E.; Klink, G. P. M. van; Vries, J. G. de; Koten, G. van *Tetrahedron* **2010**, *66*, 9009-9020.
- (64) Sperotto, E.; Klink, G. P. M. van; Vries, J. G. de; Koten, G. van *Tetrahedron* **2010**, *66*, 3478-3484.

- (65) Tornøe, C. W.; Christensen, C.; Meldal, M. *The Journal of Organic Chemistry* **2002**, *67*, 3057-64.
- (66) Rostovtsev, V. V.; Green, L. G.; Fokin, V. V.; Sharpless, K. B. *Angewandte Chemie (International ed. in English)* **2002**, *41*, 2596-9.
- (67) Díez-González, S.; Stevens, E. D.; Nolan, S. P. *Chemical Communications* **2008**, 4747-4749.
- (68) Broggi, J.; Díez-González, S.; Petersen, J. L.; Berteina-Raboin, S.; Nolan, S. P.; Agrofoglio, L. A. *Synthesis-Stuttgart* **2008**, 141-148.
- (69) Durot, S.; Mobian, P.; Collin, J.; Sauvage, J. *Tetrahedron* **2008**, *64*, 8496-8503.
- (70) Alonso, F.; Moglie, Y.; Radivoy, G.; Yus, M. *Tetrahedron Letters* **2009**, *50*, 2358-2362.
- (71) Aragão-Leoneti, V.; Campo, V. L.; Gomes, A. S.; Field, R. A.; Carvalho, I. *Tetrahedron* **2010**, *66*, 9475-9492.
- (72) Capdevielle, P.; Maumy, M. *Tetrahedron Letters* **1993**, *34*, 1007-1010.
- (73) Gujadhur, R.; Venkataraman, D.; Kintigh, J. T. *Tetrahedron Letters* **2001**, *42*, 4791-4793.
- (74) Díez-González, S.; Escudero-Adán, E. C.; Benet-Buchholz, J.; Stevens, E. D.; Slawin, A. M. Z.; Nolan, S. P. *Dalton transactions* **2010**, *39*, 7595-606.
- (75) Tubaro, C.; Biffis, A.; Scattolin, E.; Basato, M. *Tetrahedron* **2008**, *64*, 4187-4195.

Chapter 2:

The Synthesis of

Hexanuclear

Copper Clusters

2.1 The Basics of Copper

Copper adopts a variety of oxidation states from +1 to +4. Copper (III) and (IV) are relatively rare and require stabilizing ligands in order to preserve these states. Copper (III) is most commonly used in combination with copper (II) in high temperature superconductors.¹⁻³ Copper (II) is the most prevalent form of copper and is most famous for the weathered green-blue colouring on the roofs of buildings, such as, the distinctive green colour of the Parliament buildings in Canada.



Figure 2.1: Canadian Parliament building. Left image: prior to restoration, right image: post restoration^{4,5}

2.2 Copper (I)

Copper (I) is unique in itself as no other first row of the d-block metals exhibit a stable +1 oxidation state.⁶ This +1 oxidation state is of particular interest here. Solutions of copper (I) are usually colourless, but the compounds formed with copper (I) exhibit a wide range of colours depending upon the ligand environment.⁷ The chemistry of copper (I) is rich and complexes have been prepared with numerous ligands including metal-organic polymers and frameworks, metal-ligand structures and bi-metallic systems.^{2,8-19} The electronic

and photoluminescent properties of metal-organic polymers offer a variety of potential applications including luminescent materials and sensors. Important to the present work, the photoluminescent response of these polymers may be modified through changes in the metal binding environment.²⁰⁻²⁶ In addition, Figure 2.2 illustrates one of the dinuclear copper (I) complexes that can be selectively oxidized by CO₂ to form a tetranuclear copper (II) system with two CO₂ ligands bonded to each copper (II) centre. This species proceeds through a catalytic cycle that sequesters CO₂ in as lithium oxalate salts and regenerates the copper (I) precursor.^{20,27}

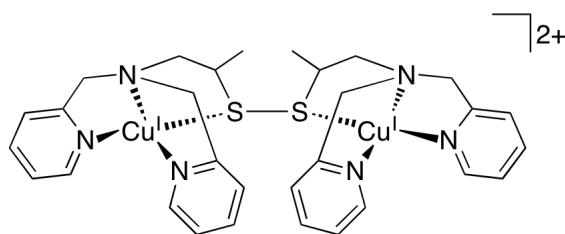


Figure 2.2: Dinuclear copper (I) complex $[Cu^I(L-L)Cu^I]^{2+}$ ($L = [N-(2-mercaptopyrpyl)-N,N-bis(2-pyridylmethyl)amine]$) used in CO₂ sequestering

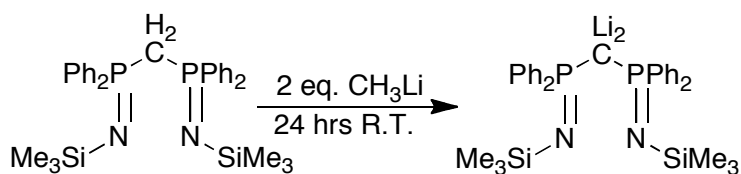
2.3 Copper Click Reactions

Another important use of copper (I) is in click reactions, described in Chapter 1. In a click reaction two reagents are combined directly in highly efficient reactions. Examples of click reactions include: the formation of C-C bonds, nucleophilic substitution, cyclo-addition.²⁸⁻⁴⁰ Copper (I) catalysts can be prepared from the reduction of copper (II) species to copper (I) either *in situ* or electrochemically. Research in the Sauvage group has shown a copper (I) complex that acts as the template for the reaction mechanism as well as the active

catalyst.^{41,42} They can also be found as pre-existing copper (I) species; as a component of a nanoparticle, in salt form or as a carbene.

2.4 The Bis(diphenyltrimethylsilyliminophosphorano)methanediide Ligand System

The dilithium salt of bis(diphenyltrimethylsilyliminophosphorano)methanediide, $[\text{Li}_2\text{C}(\text{P}=\text{NSi}(\text{CH}_3)_3)_2]_2$, herein known as **2**, was reported a decade ago by the Cavell group.^{41,42} Facile removal of the backbone protons of the methane derivative, **1**, was readily achieved upon exposure to strong bases such as alkyllithium, (e.g., phenyllithium or methyllithium; Scheme 2.1) yielding the dianion. The reduction of the methylene bridge of the ligand to a methandiide forces the two newly formed $[\text{Li}_2\text{C}(\text{Ph}_2\text{P}=\text{NSiMe}_3)_2]$, **2**, ligands to act as bilateral capping agents in a hexacopper cluster (vide infra).



Scheme 2.1: Deprotonation of bis(diphenyltrimethylsilyliminophosphorano)methane to bis(diphenyltrimethylsilyliminophosphorano)methanediide

The dimer (Figure 2.3) is made up of two ligands capped to form a cluster consisting of four lithium ions in a square planar arrangement. This assembly was

obtained via deprotonation of **1** to form dianionic methandiide salt, $[\text{Li}_2\text{C}(\text{Ph}_2\text{PNSiMe}_3)_2]$, which further condenses upon crystallization to form $[\text{Li}_2\text{C}(\text{P}=\text{NSi}(\text{CH}_3)_3)_2]_2$.

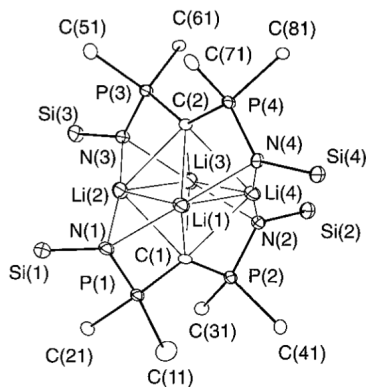


Figure 2.3: ORTEP view of $[\text{Li}_2\text{C}(\text{P}=\text{NSi}(\text{CH}_3)_3)_2]_2$, hydrogen atoms, methyl carbon atoms attached to the silicon atoms and the phenyl carbons, except the ipso-carbons have been omitted for clarity. Ellipsoids are presented at a 20% probability level⁴³

2.4.1 Computational Analysis of **1**

Density functional theory (DFT) calculations by Klobukowski et al. gave considerable insight into the formation and the stability of the Li_2L crystal. Upon condensation of the lithiated ligands, to form the dimer, the Li-C bonds lengthen while the Li-C-Li bond angle reduces by half to accommodate the distortion caused by two ligands coming close together to form the dimer. The dimer can be viewed as a carbanionic species. The electron density of the compound shifts toward the central core containing the four-lithium cluster. Pulling the molecule inward, towards the lithium cluster core, away from the outer auxiliary ligands. Lengthening of the Li-C bond distances aides in increasing the reactivity

associated with the compound **2** towards reactive precursors. The Li-Li bonds formed in organolithium compounds are typically shorter, on average 2.390 Å, than those observed for diatomic lithium (2.672 Å). The bond distance reduction is caused by a reduction in the pull of the electrons towards the nucleus, as evident from the increase in ionic character compared to that of covalency. The lithium atoms are held in close proximity via the two valence electrons in the diatomic lithium; however, the additional electronic strength donated by the anionic species of the cluster compound to the overall bond strengths associated with the Li-Li bond formation allows for the shorter bond length. As the dimer is formed there is a large change in the symmetry of the σ -bond due to the influence of the adjoining π -electron system from the ligands that is not seen in the simplistic version of a Li-cluster, mainly the example of the dilithiomethane dimer. The formation of the dimer, **2** is, overall, a favourable exothermic reaction (55 kcal/mol). Although, the initial distortion of each monomer is energy consuming the final dimerization is an exothermic process involving simultaneous distortion and dimerization.

The phosphorus-nitrogen distances lengthen to what is expected for a bond order intermediate between a single and double bond and the phosphorus-carbon bonds shorten to form more classic double bonds.⁸⁻¹¹ Thus the four membered C-P-N-M rings exhibit substantial delocalization. The formation of the complex then eloquently explains the readiness by which the carbon can be bonded to various metal centres especially as the polarity between the species increases.

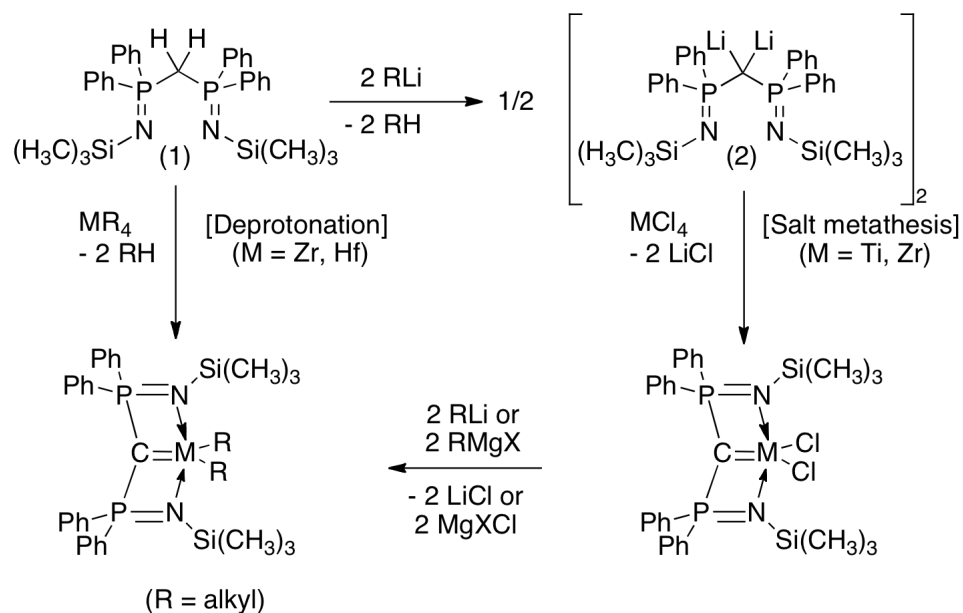
2.4.2 Sulfur-based pincer ligands

The work done on **2** has been further expanded to a related bis(diphenylthiophosphinoyl)methane ligand.⁴⁴⁻⁴⁹ Wherein, the formation of the sulfur-based dianion is achieved in the same manner as for the imino-based system, through the deprotonation of the methane protons. The ligand has the added benefit of binding well to electron-rich metal centers (i.e. palladium and rhodium) due to the use of the thiophosphinoyl ancillary ligands to form pincer complexes.

By applying a standard salt metathesis procedure in which metal ion sources and **2** were mixed, a variety of metal complexes containing the ligand may be prepared. Various researchers, including the Cavell group, have explored many reactions of compound **2** with various metals.

2.5 Reactions of 1

Deprotonation of the central carbon in compound **1** to form **2** can be achieved upon reaction with alkyl lithium reagents, as shown above in Scheme 2.1, or by using appropriate metal precursors, see Scheme 2.2.⁴³



Scheme 2.2: Reaction pathways for the formation of pincer chelates

Metal complexes of Ti, Zr and Hf were among the first metal complexes formed using either **1** or **2**. The compounds, in Figure 2.4, are two NCN pincers wherein there is a carbon metal double bond through the centre of the complex and the two imine groups flanking the metal complete the bite of the ligand to the metal.

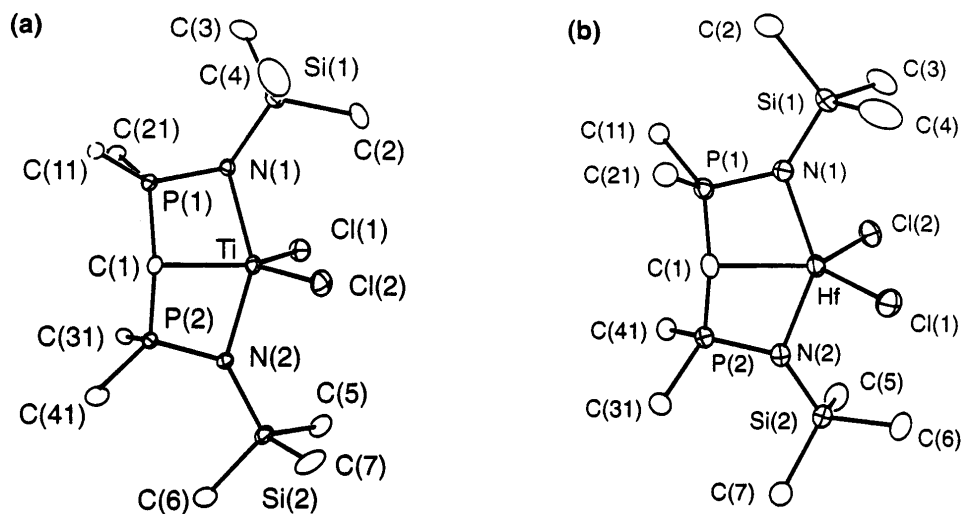


Figure 2.4: ORTEP crystal structure representations of (a) $[\text{TiCl}_2\{\text{C}(\text{Ph}_2\text{P}=\text{NSiMe}_3)_2\text{-}\kappa^3\text{C,N,N}'\}]$ and (b) $[\text{HfCl}_2\{\text{C}(\text{Cy}_2\text{P}=\text{NSiMe}_3)_2\text{-}\kappa^3\text{C,N,N}'\}]$, illustrating the isostructures. Hydrogen atoms, methyl carbon atoms attached to the silicon atoms and the phenyl carbons, except the ipso-carbons have been removed for clarity^{50,51}

To prepare complexes of hafnium or zirconium, **1** was deprotonated using an amido silyl or alkyl metal precursor. The formation of hexamethyldisilazane or alkane was achieved through the elimination of the highly acidic protons in the same way as with an alkyllithium reagent; however, high temperatures or long reaction times, between 3-7 days, were required. The synthesis could not be extended for all three group IV metals as titanium, for example, is thermally unstable in forms such as the halo-amides, alloys and simple metal. In contrast, the same reaction was performed using **2** was completed at room temperature within 1-2 days, including the titanium complex.

Another example of an attempt to access pincer complexes of platinum, specifically, with **2**, was achieved. Two equivalents of $[\text{PtCl}_2(\eta^4\text{-cod})]$ was reacted

with **2** to form $[(\eta^4\text{-cod})\text{Pt}\{\text{C}(\text{Ph}_2\text{P}=\text{NSiMe}_3)_2\text{-}\kappa\text{C},\kappa\text{N}\}]$ as a chelate in which the metal is bound to the carbene carbon atom as well as through one nitrogen atom of the ligand forming a four-membered chelate ring with the carbon, platinum and phosphorus atoms. The other half of the ligand does not coordinate, because platinum prefers to remain four coordinate, but rather remains a dangling species, as shown in Figure 2.5, which is in a fluxional state with the other nitrogen species at ambient temperatures.⁵²

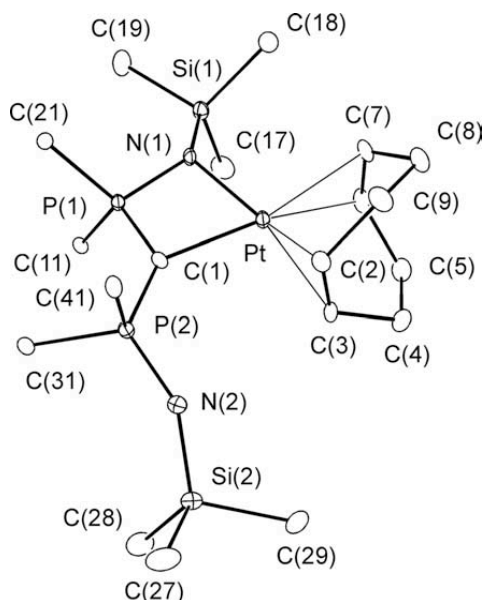
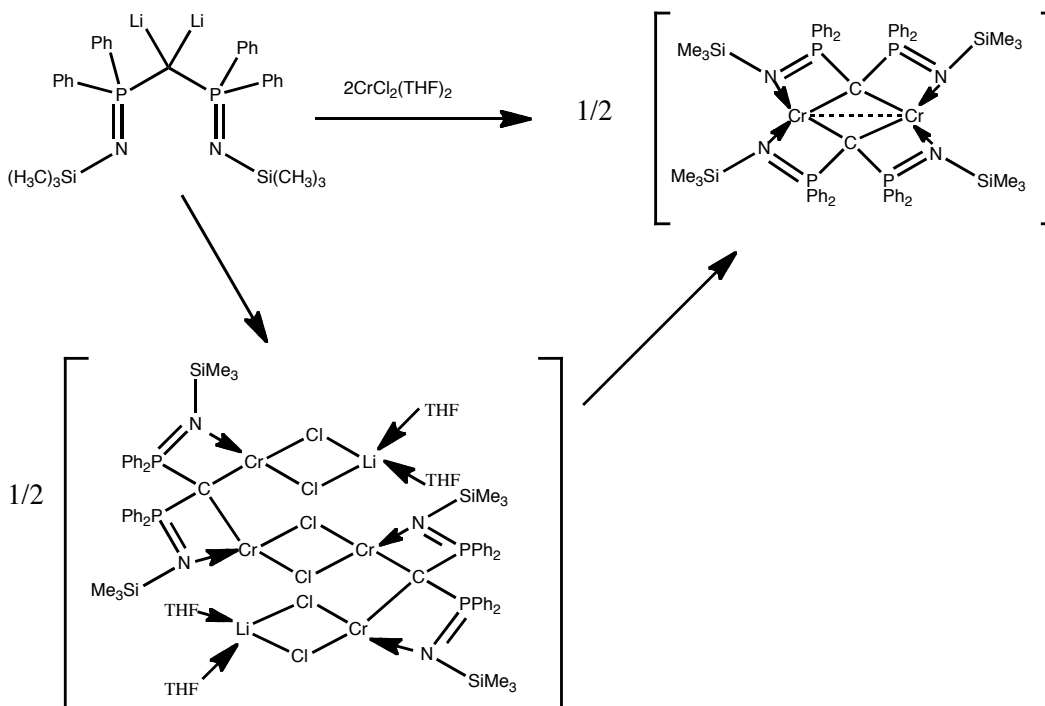


Figure 2.5: ORTEP representation of $[(\eta^4\text{-cod})\text{Pt}\{\text{C}(\text{Ph}_2\text{P}=\text{NSiMe}_3)_2\text{-}\kappa\text{C},\kappa\text{N}\}]$. Hydrogen atoms, methyl carbon atoms attached to the silicon atoms and the phenyl carbons, except the ipso-carbons have been removed for clarity⁵³

Reacting **2** with metal ions does not always afford pincer-like structures. In some cases the initial reaction forms a complicated sub-structure, such as a bridged dimer or a spirocycle. $[\text{M}_2(\mu\text{-Cl})_2\{\mu_2\text{-C}(\text{Ph}_2\text{P}=\text{NSiMe}_3)_2\text{-}\kappa^4\text{C,C',N,N'}\}(\text{LiCl})(\text{THF})_2]_2$ rearranges to form a bridged carbene complex,

$[M\{\mu_2-C(Ph_2P=NSiMe_3)_2-\kappa^4C,C',N,N'\}]_2$ as shown in Scheme 2.3; this is the case for $M = Fe, Mn, \& Cr$.^{49,53}



Scheme 2.3: Reaction of 2 with a chromium precursor to form $[Cr_2(\mu-Cl)_2\{\mu_2-C(Ph_2P=NSiMe_3)_2-\kappa^4C,C',N,N'\}(LiCl)(THF)_2\}_2$ and subsequent rearrangement to a stable form $[Cr\{\mu_2-C(Ph_2P=NSiMe_3)_2-\kappa^4C,C',N,N'\}]_2$ ^{52,54}

The remainder of this chapter will focus on the synthesis of hexanuclear copper clusters and their characterized properties. Initially the analysis will be of the optical properties observed and the related trend with respect to halide variations. The halides of interest are: chloride, bromide and iodide; however, a brief look at capping alkyl and alkoxide groups will also be discussed. A discussion on the electronic properties observed with the cluster through cyclic

voltammetry will follow the discussion of the optical properties. The chapter will close with final remarks.

2.6 Experimental

2.6.1 Materials:

All materials were purchased from Sigma-Aldrich and used as received unless otherwise specified. Azido trimethylsilane, diphenylphosphinomethane, 2,2'-bipyridine, copper (I) chloride, tri-phenyl phosphine, copper (II) bromide, and 1.4M *n*-butyl lithium in diethyl ether were purchased from Sigma-Aldrich and used as received. For cyclic voltammetry: ferrocene was purified by sublimation and tetrabutylammonium perchlorate, $\geq 99\%$ (Fluka), was used as received. Tetrahydrofuran (THF) and toluene were dried over and distilled from sodium metal, ether was obtained from an Innovative Technology, Inc. PureSolv solvent system and acetonitrile was distilled from calcium hydride.

2.6.2 General Methods:

All manipulations were performed in aerobic environments using strict Schlenk techniques or an argon-filled mBraun glove box. NMR spectra (^1H , ^{13}C , and ^{31}P) were obtained using a Varian I400 spectrometer operating at frequencies of 400, 100, and 162 MHz, respectively. Referencing for the ^1H and ^{13}C NMR spectra was done using residual solvent protons and solvent resonances, respectively. Chemical shifts for all ^{31}P NMR spectra were referenced to an 85% H_3PO_4 external solution. All NMR data was reported in parts per million (ppm)

and J coupling constants were reported in Hertz (Hz). Abbreviations for the NMR data include: s: singlet, d: doublet, t: triplet, and m: multiplet. Elemental analysis and Infrared spectroscopy data were attained through the Analytical and Instrumentation Laboratory, Department of Chemistry, University of Alberta. Mass spectroscopy analysis was carried out at the Mass Spectrometry Facility, Department of Chemistry, University of Alberta. Cyclic voltammetry was carried out using an Eplison system equipped with a RDE-2, rotating disk electrode, and a cell stand, platinum disc electrode (working electrode), a platinum wire (auxillary electrode) and an Ag/AgCl_(aq) (reference electrode). All assays were carried out in dry acetonitrile and a 0.1M tetrabutylammonium perchlorate (supporting electrode).

2.6.3 Synthetic Procedures:

Synthesis of H₂L (1**)**

25 g (0.065 mol) of diphenylphosphinomethane (CH₂(PC₆H₅)₂) was added to a flame dried three-neck 100 mL round bottom flask, fitted with a condenser and placed under an argon atmosphere. Subsequently, 25 mL (0.217 mol) of azido trimethylsilane was added while stirring and the clear yellow solution was heated at 130 °C in an oil bath for 12-16 hours. Following the precipitation of a white solid, **1**, the reaction vessel was cooled to 100 °C and placed under vacuum for 1 hr to remove the excess starting material (i.e., azido trimethylsilane). Finally, 45 mL of dry diethyl ether was added to the flask to wash and filter the product then

removed excess solvent under vacuum to leave an off-white powder. Characterization of **1** was as per literature sources.⁵⁵

Synthesis of Li₂L (**2**)

0.5 g (0.1 mmol) of **1** was placed in a 25 mL single-neck round bottom flask, fitted with a stir-bar, septum, and purge needle. Subsequently, 2 mL of dry diethyl ether was added to dissolve (**1**) affording an off-white colourless solution to which 1.87 mL (0.3 mmol) of 1.6 M methyllithium (MeLi) was added dropwise to the reaction vessel. Methane gas evolved immediately upon addition of the MeLi. The reaction mixture was stirred for 16 hours and a tan coloured precipitate formed. The solid was washed three times with diethyl ether and the solid was isolated from the diethyl ether via centrifugation in between each washing and finally dried under vacuum in the glove box. The solid must be stored in an inert argon atmosphere freezer in the glovebox. Characterization of **2**: ¹H NMR (Benzene, d₆): δ = 7.53 – 7.49 (m, phenyl), 7.04 – 6.93 (m, phenyl), 0.04 (s, CH₃Si); ¹³C {¹H} NMR (Benzene, d₆): δ = 139.0 (m, 4C, *ipso*-phenyl), 131.0 (t, ²J(P,C) = 4.5 Hz, 8C, *ortho*-phenyl), 129.0 (s, 4C, *para*-phenyl), 127.8 (s, 8C, *meta*-phenyl), 4.4 (s, 6C, CH₃Si); ³¹P {¹H} NMR (Benzene, d₆): δ = 13.7 (2P); IR (Nujol mull): 1434 (m), 1244 (s), 1190 (s), 1174 (m), 1101 (s), 1067 (s), 852 (s), 832 (s), 764 (m), 747 (m), 725 (m), 709 (m), 696 (s), 675 (w), 663 (w), 646 (s), 618 (w), 606 (w), 539, (s), 512 cm⁻¹ (m); elemental analysis calc'd for C₃₁H₃₈Li₂N₂P₂Si₂: C 65.25, H 6.71, N 4.91; found C 65.27, H 6.69, N 4.60 %.^{43,56}

Synthesis of $[\text{Cu}_6\text{Cl}_2((\text{C}_6\text{H}_5)_2\text{P}=\text{NSi}(\text{CH}_3)_3)_2]$ (**3**)

To a 20 mL vial was added 0.142 g (0.3 mmol) of $\text{Cu}_2\text{Cl}_2(\text{cod})_2$ suspended in dry THF in the glovebox. 0.166 g (0.1 mmol) of **2** was added slowly and stirred. Upon addition of **2**, the colour of the suspension changed immediately from white to deep green solution containing the final product and a green precipitate formed. The solid produced, **3**, was isolated via centrifugation and the golden-brown solution, containing the dissolved product, was reduced in volume on the vacuum line and stored under an inert atmosphere to prevent oxidation and induce crystal formation. Characterization of **3**: IR data (Nujol mull): 3074w, 3055w, 2952s, 2925s, 2855s, 1480m, 1464s, 1437m, 1377w, 1367m, 1258m, 1246s, 1103s, 1057s, 1029m, 1016m, 841s, 783s, 740s, 723m, 714w, 692s, 674m. ^1H NMR (THF- d_8): δ 8.00 (b, phenyl, 4H), 7.59 (q, phenyl, 4H), 7.44(q, phenyl, 4H), 7.30(m, phenyl, 8H), 7.12(t, phenyl, 4H), 7.01 (m, phenyl, 8H), 6.88(m, phenyl, 4H), 6.68(b, phenyl, 4H), -0.36(s, $-\text{Si}(\text{CH}_3)_3$, 18H), -0.41(s, $-\text{Si}(\text{CH}_3)_3$, 18H). $^{13}\text{C}\{^1\text{H}, ^{31}\text{P}\}$ NMR (THF- d_8): δ 137.02(s, phenyl), 136.15(s, phenyl), 135.53(s, phenyl), 134.29(s, phenyl), 133.87(s, phenyl), 133.21(s, phenyl), 132.91(s, phenyl), 132.45(s, phenyl), 130.78(s, phenyl), 130.73(s, phenyl), 130.33(s, phenyl), 130.20(s, phenyl), 128.12(s, phenyl), 128.03(s, phenyl), 5.40 (s, $-\text{Si}(\text{CH}_3)_3$), 4.21(s, $-\text{Si}(\text{CH}_3)_3$). $^{31}\text{P}\{^1\text{H}\}$ NMR (THF- d_8): δ 28.24 (P_A) and 26.17 (P_B) ($^2J_{A-B} = 56.0$ Hz.). ESI-MS (THF+Toluene): m/z 1565.9 $[\text{M}+\text{H}]^+$. Anal. Calc'd for $\text{C}_{62}\text{H}_{76}\text{N}_4\text{P}_4\text{Si}_4\text{Cl}_2\text{Cu}_6(\text{C}_4\text{H}_{10}\text{O})_2$: C, 49.05; H, 5.61; N, 3.27. Found: C, 49.29; H, 5.68; N, 3.33 %. (^1H NMR in THF- d_8 also detected the two ether molecules.).⁵⁷

Synthesis of $[\text{Cu}_6\text{Br}_2((\text{C}_6\text{H}_5)_2\text{P}=\text{NSi}(\text{CH}_3)_3)_2]$ (**4**)

To a 20 mL vial 0.142 g (0.3 mmol) of $\text{Cu}_2\text{Br}_2(\text{cod})_2$ was added and suspended in dry THF. 0.166 g (0.1 mmol) of **2** was added slowly and stirred. Upon addition of the **2** the colour of the suspension changed immediately from white to deep green solution containing the product and a green-brown precipitate formed. The product was isolated via centrifugation and the golden-brown solution was reduced in volume on the vacuum line and stored under an inert atmosphere to induce crystal formation. Characterization of **4**: IR data (Nujol mull): 3073m, 3048m, 2951s, 2895s, 1481m, 1436s, 1398w, 1307w, 1246s, 1180w, 1101s, 1061s, 1028m, 1010m, 832s, 785s, 769s, 741m, 722w, 692s, 673m. ^1H NMR(THF- d_8): δ 7.72 (m, phenyl, 8H), 7.58 (q, phenyl, 4H), 7.48(q, phenyl, 4H), 7.39(m, phenyl, 4H), 7.32(t, phenyl, 8H), 7.12 (m, phenyl, 4H), 7.01(m, phenyl, 4H), 6.91(m, phenyl, 4H), -0.26(s, $-\text{Si}(\text{CH}_3)_3$, 18H), -0.30(s, $-\text{Si}(\text{CH}_3)_3$, 18H). $^{13}\text{C}\{^1\text{H}\}$ NMR (THF- d_8): δ 136.82(d, phenyl), 135.82(d, phenyl), 133.83(d, phenyl), 132.85(d, phenyl), 132.54(t, phenyl), 131.65(s, phenyl), 130.80(s, phenyl), 130.33(d, phenyl), 129.20(s, phenyl), 128.83(t, phenyl), 128.09(t, phenyl), 5.43 (d, $\text{Si}(\text{CH}_3)_3$), 4.26(d, $\text{Si}(\text{CH}_3)_3$). $^{31}\text{P}\{^1\text{H}\}$ NMR (THF- d_8): δ 28.10 (P_A) and 26.59 (P_B) ($^2J_{\text{A-B}} = 57.0$ Hz.). ESI-MS (THF+Toluene): m/z 1653.8 $[\text{M}+\text{H}]^+$. Anal. Calc'd for $\text{C}_{62}\text{H}_{76}\text{N}_4\text{P}_4\text{Si}_4\text{Br}_2\text{Cu}_6$: C, 45.01; H, 4.60; N, 3.38. Found: C, 45.10; H, 4.63; N, 3.36 %.⁵⁷

Synthesis of $[\text{Cu}_6\text{I}_2((\text{C}_6\text{H}_5)_2\text{P}=\text{NSi}(\text{CH}_3)_3)_2]$ (**5**)

0.142 g (0.3 mmol) of $\text{Cu}_2\text{I}_2(\text{cod})_2$ was added to a 20 ml vial and suspended in dry THF in the glove box to which 0.166 g (0.1 mmol) of solid **2** was added slowly with stirring. Upon addition of **2**, the colour of the suspension changed immediately from white to golden-brown colour solution, containing the product, with a green-brown precipitate. The product containing solution was isolated from the solids via centrifugation. The golden-brown solution was reduced in solvent volume on the vacuum line to recover the solid product (**5**) and stored under an argon atmosphere in the glovebox freezer to induce crystallization. Characterization of **5**: IR data (Nujol mull): 3047w, 2930s, 2856s, 1465s, 1437m, 1377m, 1367m, 1257m, 1245s, 1102s, 1078s, 1061s, 1029m, 832s, 777s, 751s, 737m, 713m, 692s, 672m. ^1H NMR(THF- d_8): δ 7.77 (q, phenyl, 4H), 7.61 (q, phenyl, 4H), 7.52(q, phenyl, 4H), 7.44(m, phenyl, 4H), 7.36(t, phenyl, 4H), 7.28 (t, phenyl, 4H), 7.13(m, phenyl, 4H), 7.05(m, phenyl, 4H), 6.98(m, phenyl, 4H), 6.92(m, phenyl, 8H), -0.22(s, -Si(CH₃)₃, 18H), -0.29(s, -Si(CH₃)₃, 18H). $^{13}\text{C}\{^1\text{H}\}$ NMR (THF- d_8): δ 138.05(d, phenyl), 137.22(d, phenyl), 136.84(d, phenyl), 136.06(d, phenyl), 135.62(d, phenyl), 134.73(d, phenyl), 134.06(d, phenyl), 133.76(d, phenyl), 133.26(d, phenyl), 132.75(q, phenyl), 130.84(d, phenyl), 130.35(d, phenyl), 129.13(br, t, phenyl), 128.15(m, phenyl), 5.43 (d, -Si(CH₃)₃), 4.34(d, -Si(CH₃)₃). $^{31}\text{P}\{^1\text{H}\}$ NMR (THF- d_8): δ 28.95 (P_A) and 28.08

(P_B) (²J_{A-B} = 56.0 Hz.). ESI-MS (THF+Toluene): *m/z* 1747.8 [M+H]⁺. Anal. Calc'd for C₆₂H₇₆N₄P₄Si₄I₂Cu₆ 1/2(C₄H₁₀O): C, 43.05; H, 4.57; N, 3.14. Found: C, 43.03; H, 4.55; N, 3.18 %.⁵⁷

Synthesis of Cu₂Cl₂(bipy)₂

In an argon-filled glovebox 0.156 g (1.0 mmol) of 2,2'-bipyridine was dissolved in dry acetone along with 0.098g (1.0 mmol) of CuCl. Upon dissolution a deep red-brown solution formed and some red-brown precipitate was observed. The product was isolated via centrifugation. Acetone was removed from the sample on the vacuum line in the glovebox and the red-brown product was washed with dry ether and a crystalline compound was recovered. Characterization was as per literature source.^{58,59}

Synthesis of CuBr(PPh₃)₃

In an Erlenmeyer flask 100 mL of boiling methanol containing 6.12 g (23.3 mmol) of PPh₃ was added 1.87 g (8.36 mmol) of CuBr₂, slowly. As the reaction mixture was stirred the colour changed from dark black-green to reddish colour and a white solid precipitate was observed. The white solid was filtered using a Buchner funnel and washed three times with 95% ethanol, then diethyl ether and then the solvent was removed and the product dried under high vacuum. Yield was 70 %. Characterization was as per literature sources.¹⁷

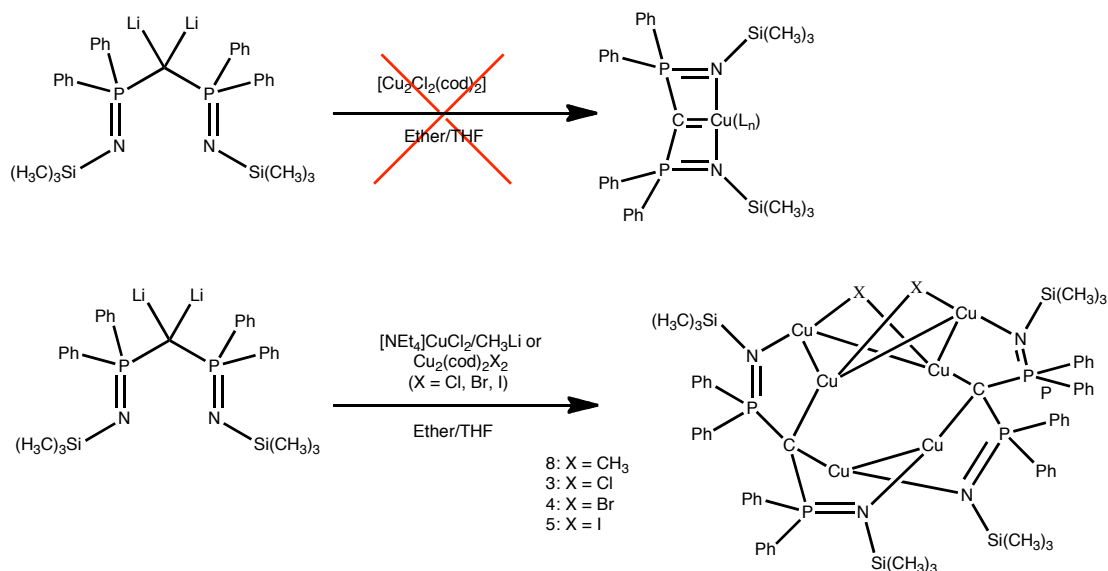
Synthesis of $[\text{CuCl}(\text{cod})]_2$

1.943 g of $\text{CuCl}_{(s)}$ (19.6 mmol) was added to 5.5 mL of 1,5-cyclooctadiene (cod) (44.7 mmol) in 50 mL of 0.18 M HCl. The reagents were shaken together for 10 minutes upon which the sample solution became a clear blue with white solids floating atop the solution. The white solids, $[\text{CuCl}(\text{cod})]_2$, were collected via vacuum filtration and washed three times with distilled water and n-pentane, respectively. Characterization was as per literature sources.^{60,61}

2.7 Results and Discussion

2.7.1 Copper reactions with Li_2L

One of the goals of the present work is the study of the hexanuclear copper clusters. Initially the reaction of **2** with a copper (I) precursor was expected to yield a NCN pincer complex with a copper atom bonded to the carbon atom in the backbone the ligand (See Scheme 2.4).



Scheme 2.4: Adapted pincer scheme for the reaction of Li_2L and $[\text{Cu}_2\text{Cl}_2(\text{cod})_2]$ (top), actual hexanuclear copper cluster scheme (bottom)

Surprisingly, pincer complexes were not isolated; instead chelates and multi-nuclear copper clusters were obtained (Scheme 2.4). Other hexanuclear copper clusters have been prepared starting with copper (II) precursors; however, this system was the first to yield a cluster of this type starting with copper (I) precursor.

In 2003, Sandor *et al.* determined the presence of copper (II) ions, quantitatively, by forming a highly luminescent hexanuclear copper (I) cluster in a variety of media. Upon complexation with N-ethyl-N'-methylsulfonylthiourea the copper (II) complexes undergo a set of reduction-oxidation reactions where the ligand is oxidized as a counterpart to copper (II) being reduced to copper (I). The copper (I) complexes then aggregate together to form the luminescent copper (I) hexaclusters, see Figure 2.6. In contrast to the iminophosphorano clusters of **2**, the

hexa-copper framework is quasi-octahedral with chelate bridges. These clusters have been proposed as active species in luminescent sensing of various environmental analytes.⁵³

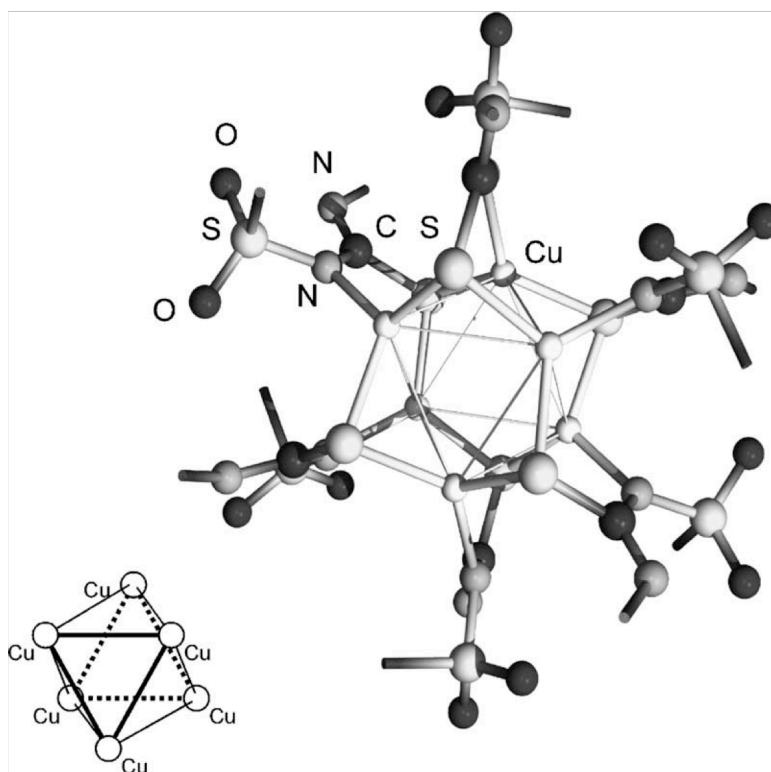


Figure 2.6: Distorted hexanuclear copper cluster for the determination of copper (II) ions⁶⁵

The clusters, **3-5**, were prepared by reacting **2** with $\text{Cu}_2\text{X}_2(\text{cod})_2$ where $\text{X} = \text{Cl}, \text{Br}$ or I , in a 1:3 molar ratio in dry THF.⁶³ Upon the addition of the precursor the reaction mixture changed colour and a white precipitate formed. The products, compounds **3**, **4** or **5** in solution, were isolated via centrifugation to separate the precipitate and solvent content was reduced using a vacuum line housed within an argon-filled glovebox. Samples were isolated and identified using ^{31}P NMR.

Interestingly, compound **8**, could be indirectly formed by reacting **3** with LiCH_3 as a compliment to the direct method of reacting **2** with $\text{NEt}_4\text{CuCl}_2/\text{LiCH}_3$.

The hexanuclear copper clusters were characterized via X-ray crystallography; the copper atoms assemble in a boat conformation, see Figure 2.7. Based upon the Cu-Cu distances (i.e., 2.4000(4) – 2.9458(5) Å) the copper atoms are joined through multiple Cu-Cu bonds. Each of the two pincer ligands bond two of the copper atoms, forming the base of the boat, through geminal bonds with the backbone carbon atom from compound **2**, the additional four Cu atoms are linked through Cu-Cu bonds as well as through coordination with the nitrogen atoms of the ligand.

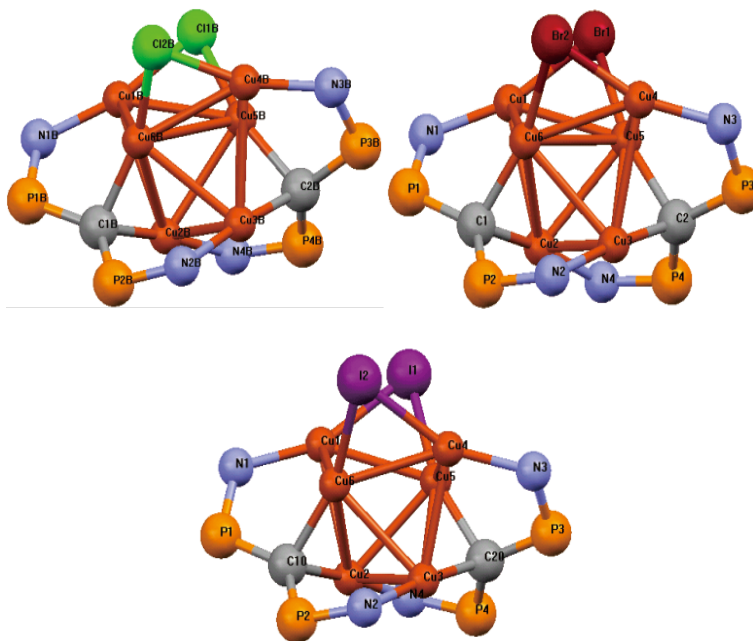


Figure 2.7: Core structures of the hexanuclear copper clusters (3) left, (4) middle and (5) right⁵⁷

The halides bridge the two copper atoms at the top of the boat formation. Interchanging the halide caps from chloride through to iodide forms compounds, which are isosymmetric to each other. The bond distances vary with the halide size, in that, the caps increase in size from chloride to iodide. As a consequence, of the cap size enlargement, the Cu-Cu bond distances decrease causing a change in the observed luminescent properties.

2.7.2 Photoluminescent Properties of Hexanuclear Copper Clusters

UV-vis absorption spectra of five different solutions can be seen in Figure 2.8. The compounds **3-5** are as previous; however, compound **7** and **8** are the iodide chelate, $[\text{CuI}(\text{C}_6\text{H}_5)_2\text{P}=\text{NSi}(\text{CH}_3)_3)_2]$ and $[\text{Cu}_6(\text{CH}_3)_2((\text{C}_6\text{H}_5)_2\text{P}=\text{NSi}(\text{CH}_3)_3)_2]$ cluster, respectively. As the halide cap is changed from chloride to bromide to iodide there is a slight observed red-shift in optical absorbance. The red shift can be attributed to halide-metal charge transfers (XMCT).⁶⁶ The absorbance spectra of **7** and **8** are also shown in Figure 2.8. The spectrum of **8** is similar to that of the hexanuclear copper-halide clusters indirectly suggesting the formation of a hexanuclear cluster. The spectrum of compound **7** does not show the same spectral features as **3-5** presumably because it is not a cluster. Compound **7** appears as an outlier; however, as it is a chelate the pronounced blue-shift in the absorbance is reasonable and has also been attributed to XMCT.^{65,67,68}

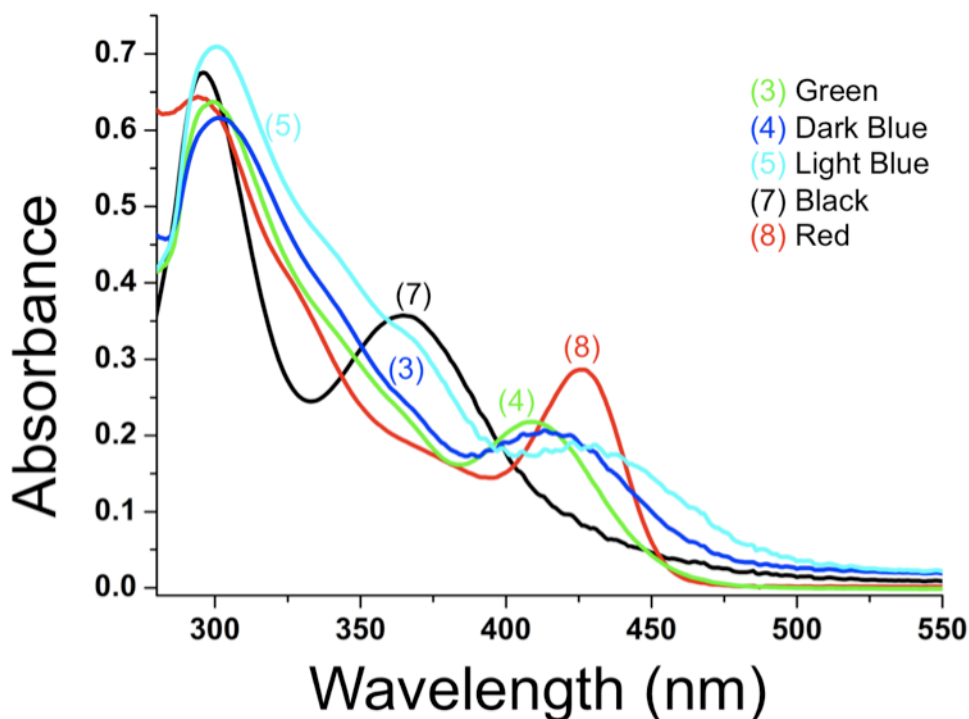


Figure 2.8: UV-Visible absorbance spectra for compounds: (3) $[\text{Cu}_6\text{Cl}_2((\text{C}_6\text{H}_5)_2\text{P}=\text{NSi}(\text{CH}_3)_3)_2]_2$, (4) $[\text{Cu}_6\text{Br}_2((\text{C}_6\text{H}_5)_2\text{P}=\text{NSi}(\text{CH}_3)_3)_2]_2$, (5) $[\text{Cu}_6\text{I}_2((\text{C}_6\text{H}_5)_2\text{P}=\text{NSi}(\text{CH}_3)_3)_2]_2$, (7) $[\text{CuI}(\text{C}_6\text{H}_5)_2\text{P}=\text{NSi}(\text{CH}_3)_3]_2$, and (8) $[\text{Cu}_6(\text{CH}_3)_2((\text{C}_6\text{H}_5)_2\text{P}=\text{NSi}(\text{CH}_3)_3)_2]^{57}$

The hexanuclear copper cluster photophysical properties are as follows. From the absorption spectra, coupled with DFT calculations it was suggested that the large bands in the UV range for compounds **3**, **4** and **5** are attributable to $3d \rightarrow 4p$ transitions through the metal centres of the copper clusters. The other main peaks, in the near-visible region, 409, 413 and 423 nm, were attributed to a combination of ligand to metal charge transfer (LMCT) and metal centered $d \rightarrow s$ transitions.⁶⁹ The weak shoulders around 360 nm were assigned as XMCTs in the spectra of the three halide capped clusters were supported by compounds **8** and **7**; the fact that compound **8** has no representation of a shoulder peak indicates that

the transition is due to a halide-metal or halide-ligand interaction. Compound **7**, possessing one halide, supports the XMCT as the halide is directly bonded to the copper atom in a manner which does not allow optimal orbital overlap for the required electronic transitions for XLCT. The cluster luminescence, however, can be attributed to many different factors, including, for example, the substituents on the ligands. Energy from the diphenyl substituents lessens the likelihood for luminescence, as the emission energies of intra-ligand excited states are low. Often the phenomenon of luminescence can be attributed to MLCT; unfortunately, copper (I) tends to reduce as opposed to oxidize. This indicates the copper has a preference to gain an electron in the 4s orbital than to lose one forcing the orbital occupation from $3d^{10}$ to $3d^9$. A report by Vogler *et al.* postulated that due to the common luminescence observed in various copper clusters with different ligands, the transitions are likely not due to charge transfers from the metal to the ligand.⁷⁰⁻⁷² More accurately the excitation and consequent relaxation can be related to $s \rightarrow d$ transitions as opposed to the $d-\pi^*$ charge transfers associated with a metal to ligand charge transfer.

The emission spectra, Figure 2.9, compliments the absorption spectra nicely, the $s \rightarrow d$ transitions account for the emissive aspect of compound **8** while the hexanuclear copper clusters can attribute their emission to d-s and/or XMCT delocalized character over the copper cluster core as well as the d-s and/or XLCT characteristics of the clusters attributing to the high energy shoulder peaks. The $s \rightarrow d$ transitions are due to an excited state of the copper metal where the configuration $3d^9 4s^1$ was proposed to be caused by the copper-copper metal

interactions and thus can not be extrapolated to the mononuclear copper chelate formation, which is also the reason for the absence of a shoulder in the emission spectrum of **7**. Due to steric constraints, put in place by the increasing size of halide ligands, the bonds between copper atoms shortens, increasing the cuprophilic interactions. The overlap of the 4s and 4p orbitals causes an overall gain in the bonding character through the filled d-orbitals; thereby, allowing transitions from a filled anti-bonding d-orbital to a higher energy empty s-orbital. The red-shift observed for compounds **3-5** are consistent with the change in electronic transition abilities within the clusters.^{17,60,61,73}

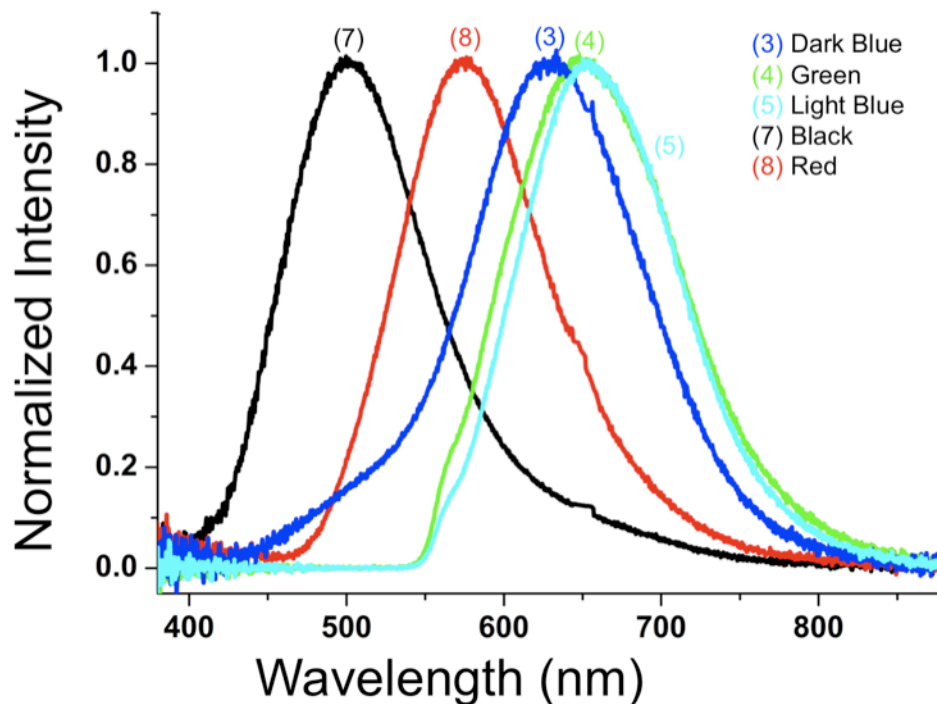


Figure 2.9: Photoluminescence emission spectra for compounds: (3) $[\text{Cu}_6\text{Cl}_2((\text{C}_6\text{H}_5)_2\text{P}=\text{NSi}(\text{CH}_3)_3)_2]_2$, (4) $[\text{Cu}_6\text{Br}_2((\text{C}_6\text{H}_5)_2\text{P}=\text{NSi}(\text{CH}_3)_3)_2]_2$, (5) $[\text{Cu}_6\text{I}_2((\text{C}_6\text{H}_5)_2\text{P}=\text{NSi}(\text{CH}_3)_3)_2]_2$, (7) $[\text{CuI}(\text{C}_6\text{H}_5)_2\text{P}=\text{NSi}(\text{CH}_3)_3]_2$, and (8) $[\text{Cu}_6(\text{CH}_3)_2((\text{C}_6\text{H}_5)_2\text{P}=\text{NSi}(\text{CH}_3)_3)_2]_2$. Excitation was done through a 325 nm He-Cd laser⁵⁷

2.7.3 Photoluminescent Properties of Hexanuclear Copper Clusters Beyond Halides

Copper clusters in the literature have shown variability in their observed luminescence due to the choice of reactants and/or ligands. The noted photoluminescent colour of the hexanuclear copper clusters with the halide caps were typically bright red-orange. Upon further reaction of compound **3** with NaO^tBu a change in the colour emitted under a UV-lamp was observed as well as

a consequential change in the AB coupling constants and chemical shift in the ^{31}P NMR spectrum. The compound had a green emission under UV exposure, thus changing the optical properties in such a direct manner was deemed highly desirable and propelled the research in a direction to attempt to understand the effects of reactions with various chalcogenides.

2.7.4 Electrochemical Analysis of the Ligands and the Hexanuclear Copper Clusters

Electrochemical data can give information regarding the potential activity of a chemical species in catalytic cycles. Cyclic voltammetry offers insight into the formation of various species that are electrochemically generated at the surface of an electrode.^{71,74-76} The proposal that hexanuclear copper cluster species could show catalytic activity stems from the discovery that the complex $[\kappa\text{C},\kappa\text{C},\kappa\text{N},\kappa\text{N}']\text{-}\{(\text{Me}_3\text{SiN}=\text{P}(\text{Ph})_2)_2\text{C}\}(\text{Me}_2\text{Al})_2$, seen in Figure 2.10, shows catalytic activity toward olefin polymerization.⁷⁷ The dinuclear aluminum complex showed higher activity than mononuclear species; therefore, while mono-copper complexes may show catalytic activity it may be possible to increase catalytic activity through the use of a hexanuclear copper complex with accessible reaction sites.

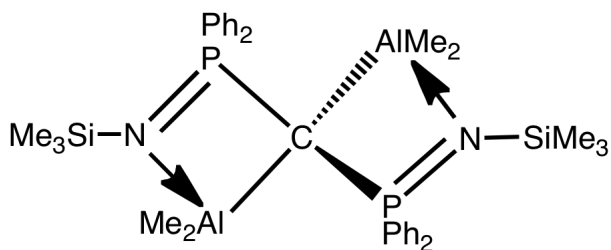


Figure 2.10: Aluminum catalyst for olefin polymerization [$\kappa C, \kappa C, \kappa N, \kappa N'$ - $\{(Me_3SiN=P(Ph)_2)_2C\}(Me_2Al)_2]$

To better understand the reduction-oxidation (redox) properties of the present hexacopper compounds, cyclic voltammetry was performed. This three-electrode method introduces a controlled electrical current across a series of electrodes, a working and reference electrode in this case, to which the change in potential can be determined through a measured current between the working and counter electrode. The analysis allows for the determination of reversibility, irreversibility or quasi-reversibility of redox processes.⁷⁸

For completeness, initial cyclic voltammetry studies outlined here evaluated the redox activity of ligands **1** and **2**. Representative cyclic voltammograms are shown in Figures 2.11 and 2.12. These graphs indicate ligands **1** and **2** are not electroactive. Any passage of current noted in the following cyclic voltammograms arise from the electrolyte medium, which was run independently for comparison purposes.

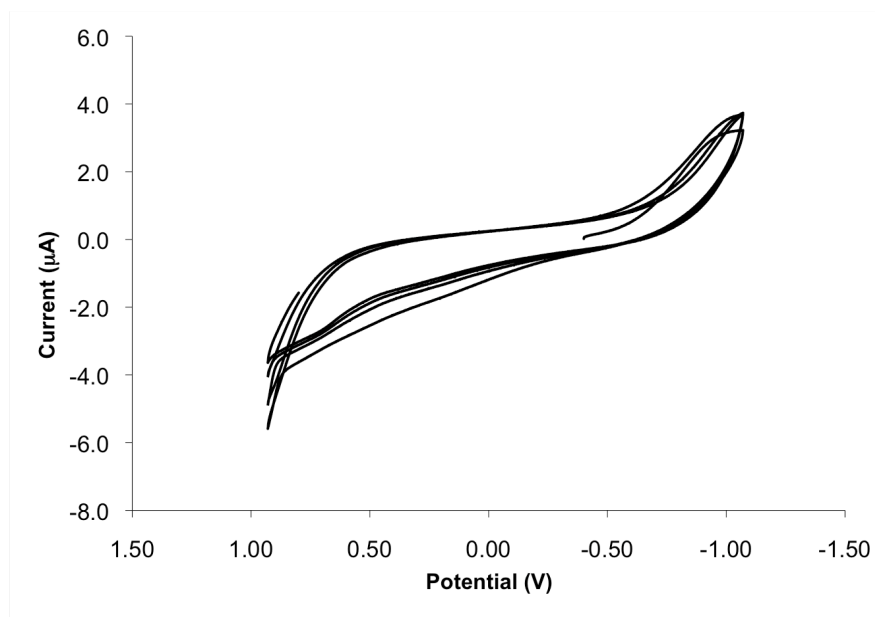


Figure 2.11: Cyclic voltammogram of **1** in dry, deaerated acetonitrile and 0.1 M tetrabutyl ammonium perchlorate as supporting electrolyte at a scan rate of 50 mV/s at 25°C. Standardized to Fc^+/Fc

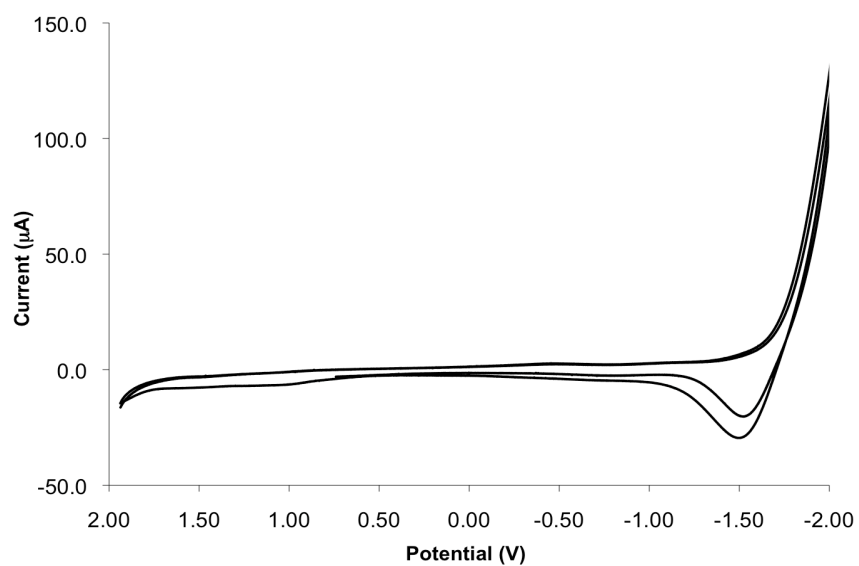


Figure 2.12: Cyclic voltammogram of compound **2** in dry acetonitrile and 0.1 M tetrabutyl ammonium perchlorate as supporting electrolyte at a scan rate of 50 mV/s at 25°C. Standardized to Fc^+/Fc

The cyclic voltamograms of **3**, **4**, and **5** are shown in Figures 2.13-2.15. The hexanuclear copper clusters with halide caps show an intense irreversible peak was observed at -0.25 eV in the reductive cycle. This feature was assigned to a stripping peak, which arises from copper (I) being reduced to metallic copper (0) and depositing on the electrode surface. When the polarity of the electrode is changed to an oxidizing potential current passes and the copper (0) film is converted to copper (I) and stripped off the electrode. The area under this feature increases with increasing scans because the copper (0) film being deposited is not completely removed during the oxidative scan resulting in a build up of the copper film. Because copper is conductive the area of the electrode and hence the current passed increases.^{79,80}

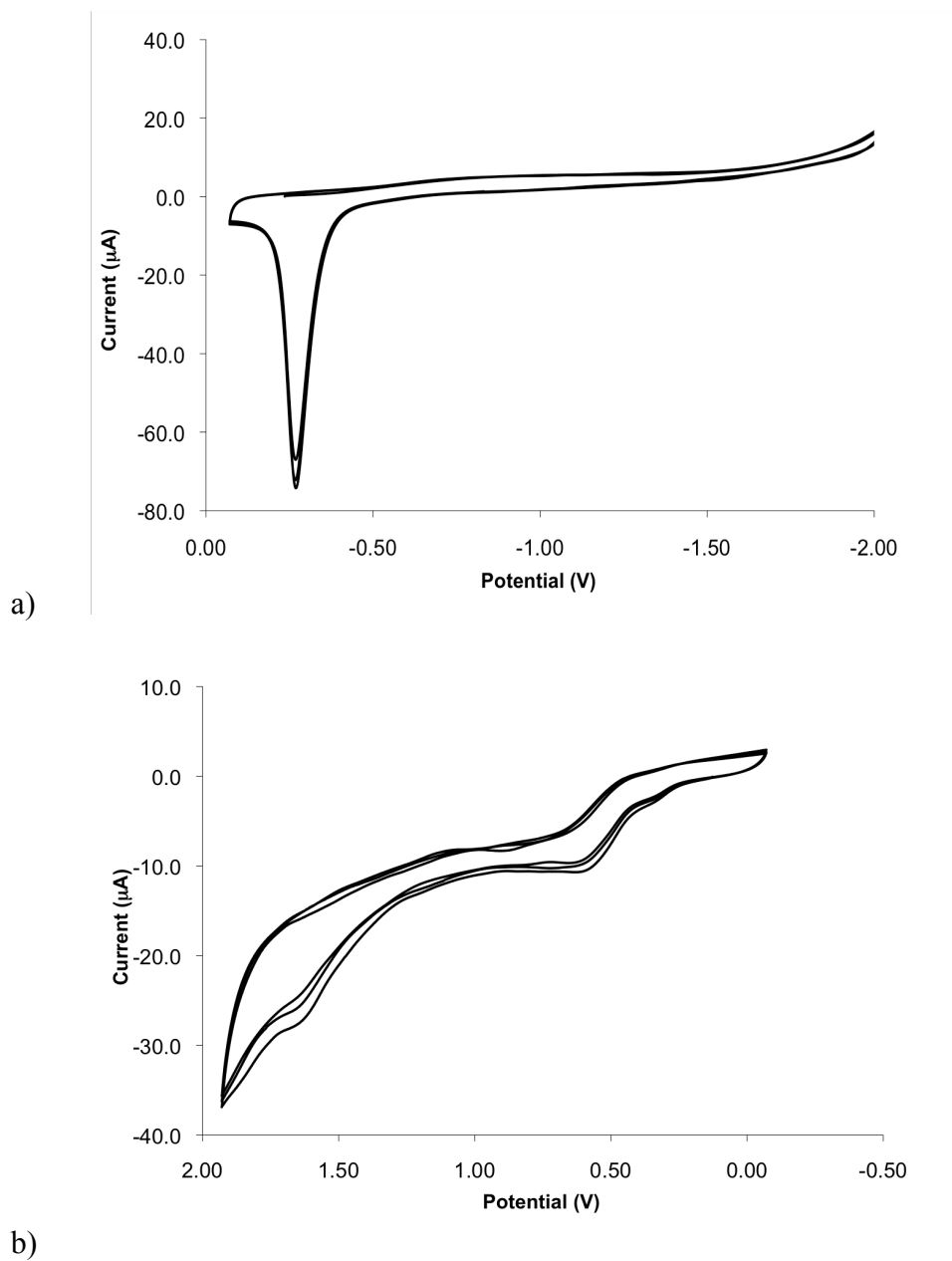
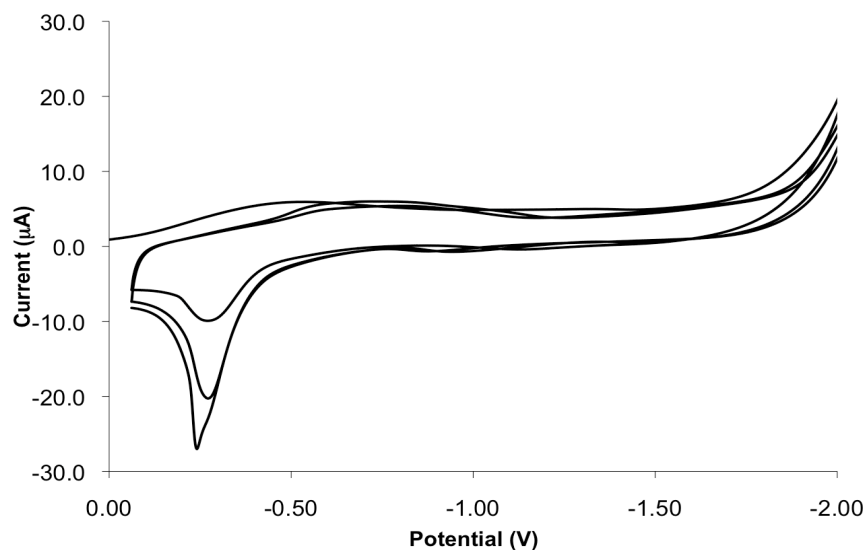
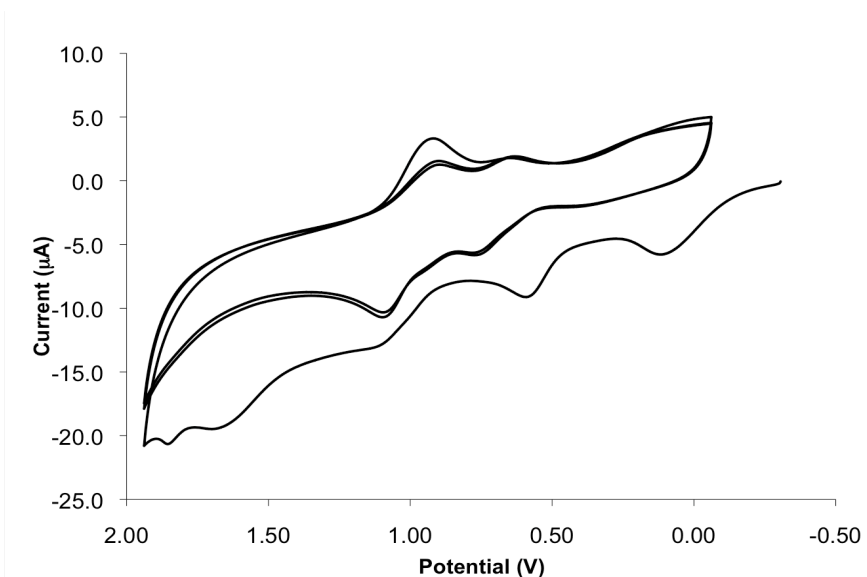


Figure 2.13: Cyclic voltammogram of **3** in dry acetonitrile and 0.1 M tetrabutyl ammonium perchlorate as supporting electrolyte at a scan rate of 50 mV/s at 25°C. Standardized to Fc^+/Fc . a) reductive cycle b) oxidative cycle

Two features are notable in the oxidative scans of the copper clusters (Figure 2.13) two peaks were observed of which one was irreversible and the other can be observed as reversible.



a)



b)

Figure 2.14: Cyclic voltammogram of 4 in dry acetonitrile and 0.1 M tetrabutyl ammonium perchlorate as supporting electrolyte at a scan rate of 50 mV/s at 25°C. Standardized to Fc^+/Fc . a) reductive cycle b) oxidative cycle

In Figure 2.14 the stripping peak can be seen in Figure 2.14 a) during the reductive cycle. In the oxidative cycle, Figure 2.14 b), a few peaks were observed. Peaks at 0.060, 0.726 and 1.056 V indicate a reaction in which the copper (I)

atoms are oxidized to copper (II) atoms but the reversibility of the atoms is not consistent, as shown by the reverse peaks at 0.640 and 0.912 V being visible but not consistent.

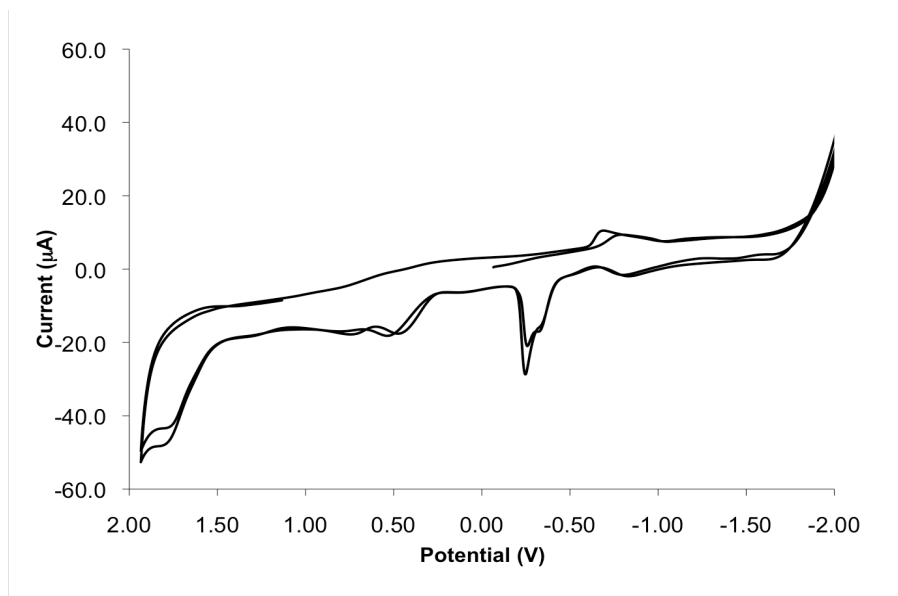


Figure 2.15: Cyclic voltammogram of compound **5** in dry acetonitrile and 0.1 M tetrabutyl ammonium perchlorate as supporting electrolyte at a scan rate of 50 mV/s at 25°C. Standardized to Fc^+/Fc

The compound **5** has a cyclic voltammogram, as seen in Figure 2.15, which shows the stripping peak and a reversible peak in the reduction of copper (I) atoms to copper (0) atoms. Reductively speaking, the observable peaks are irreversible in nature.

The information attained from the cyclic voltammograms sheds light onto whether or not the clusters would be applicable in a catalytic setting. The clusters show reduction-oxidation characteristics; however, due to the fact that the curve changes upon sequential current passes indicates that the clusters may be changing composition irreversibly. Thus, as a catalytic precursor, the applications

would be limited because of the lack of flexibility within the system to replenish the six copper (I) atoms within the original structure (i.e. the oxidative cycles, from copper (I) to copper (II)). It appears that after the first cycle of redox potentials the cluster changes to a more stable format after which the cycles become consistent but still most of the peaks are irreversible. Research by Gamelas *et al.* illustrates the change in structure as well as the irreversible aspect in the oxidative side of the potential spectrum. Further to the discussion is the observation that only one peak is observed in the spectrum whereas in the cluster case more than one irreversible peak is visible; however, not all six clusters were observed individually in each spectra. Studies have shown that as copper (I) is oxidized to copper (II) its geometry changes from tetrahedral with respect to the copper atoms to a pseudo-tetrahedral, which can be attributed to the observed change in the curve upon sequential changes in potentials.^{81,82} The cyclic voltammetry data does not conclusively indicate whether or not the hexanuclear complexes are viable for catalytic precursors, but rather, does indicate that the clusters are capable of conducting electrical currents. Therefore, the use of the cluster in a catalytic setting is left to be determined through the attempt of known catalytic reactions.

2.8 Conclusions

The hexanuclear clusters formed were characterized through optical and electrochemical channels. The photoluminescent properties showed variety through the ligands chosen for the copper cluster formation, while the

electrochemical data attained indicated that the catalytic viability could be possible, however, limited. Chapter 3 will explore variance in the hexanuclear cluster caps in an attempt to form a sensor-like compound.

2.9 References

- (1) Sousa, J.; Luiz, A.; Vugman, N. *Journal of Magnetism* **2001**, 226-230, 309-310.
- (2) Lampeka, Y. *Polyhedron* **2000**, 19, 2533- 2538.
- (3) Khan, M. *Journal of Inorganic and Nuclear Chemistry* **1972**, 34, 3591-3593.
- (4) http://peace.maripo.com/p_ww_i.htm.
- (5) <http://stopthecap.com/wp-content/uploads/2011/02/canadianparliament.jpg>.
- (6) Housecroft, C. E.; Sharpe, A. G. *Inorganic Chemistry 2nd edition*; 2nd ed.; Pearson Education Limited: Harlow, England, 2005; pp. 1-949.
- (7) Altaf, M.; Stoeckli-Evans, H. *Inorganica Chimica Acta* **2010**, 363, 2567-2573.
- (8) Lazarou, K.; Bednarz, B.; Kubicki, M.; Verginadis, I. I.; Charalabopoulos, K.; Kourkoumelis, N.; Hadjikakou, S. K.; Verginadis II *Inorganica Chimica Acta* **2010**, 363, 763-772.
- (9) Dhillon, H.; Sharma, K.; Gehlot, R.; Kumbhat, S. *Electrochemistry Communications* **2009**, 11, 878-880.
- (10) Rapisarda, V. A; Volentini, S. I.; Fariás, R. N.; Massa, E. M. *Analytical Biochemistry* **2002**, 307, 105-9.
- (11) Jeuken, L. J.; Ubbink, M.; Bitter, J. H.; Vliet, P. van; Meyer-Klaucke, W.; Canters, G. W. *Journal of Molecular Biology* **2000**, 299, 737-55.
- (12) Sperotto, E.; Klink, G. P. M. van; Vries, J. G. de; Koten, G. van *Tetrahedron* **2010**, 66, 9009-9020.
- (13) Nakamura, E.; Mori, S. *Angewandte Chemie International Edition* **2000**, 39, 3750-3771.
- (14) Jin, Q.-H.; Xiao, Y.-L.; Hu, K.-Y.; Li, Z.-F.; Wang, R.; Zhang, C.-L. *Inorganic Chemistry Communications* **2011**, 2, 2-6.
- (15) Cauzzi, D.; Graiff, C.; Lanfranchi, M.; Predieri, G.; Tiripicchio, A. *Chemical Communications* **1995**, 0, 2443-2444.

- (16) Brooker, S.; Davidson, T. C.; Hay, S. J.; Kelly, R. J.; Kennepohl, D. K.; Plieger, P. G.; Moubaraki, B.; Murray, K. S.; Bill, E.; Bothe, E. *Coordination Chemistry Reviews* **2001**, 216-217, 3-30.
- (17) Bowmaker, G. A.; Jirong, W.; Hart, R. D.; White, A. H.; Healy, P. C. *Journal of the Chemical Society, Dalton Transactions* **1992**, 787.
- (18) Beletskaya, I. P.; Cheprakov, A. V. *Coordination Chemistry Reviews* **2004**, 248, 2337-2364.
- (19) Connelly, N. G.; Geiger, W. E. *Chemical Reviews* **1996**, 96, 877-910.
- (20) Zhang, J.; Xue, Y.-S.; Li, Y.-Z.; Du, H.-B.; You, X.-Z. *CrystEngComm* **2011**, 13, 2578-2585.
- (21) Heller, M.; Sheldrick, W. S. *Zeitschrift für anorganische und allgemeine Chemie* **2004**, 630, 1869-1874.
- (22) Kim, T. H.; Lee, K. Y.; Shin, Y. W.; Moon, S.-T.; Park, K.-M.; Kim, J. S.; Kang, Y.; Lee, S. S.; Kim, J. *Inorganic Chemistry Communications* **2005**, 8, 27-30.
- (23) Kim, T. H.; Shin, Y. W.; Jung, J. H.; Kim, J. S.; Kim, J. *Angewandte Chemie (International ed. in English)* **2008**, 47, 685-8.
- (24) Kitagawa, S.; Kondo, M. *Bulletin of the Chemical Society of Japan* **1998**, 71, 1739-1753.
- (25) Lee, J. Y.; Lee, S. Y.; Sim, W.; Park, K.-min; Kim, J.; Lee, S. S. *Journal of the Chemical Society-Chemical Communications* **2008**, 1, 6902-6903.
- (26) Peindy, H. N.; Guyon, F.; Khatyr, A.; Knorr, M.; Strohmann, C. *European Journal of Inorganic Chemistry* **2007**, 2007, 1823-1828.
- (27) Angamuthu, R.; Byers, P.; Lutz, M.; Spek, A. L.; Bouwman, E. *Science (New York, N.Y.)* **2010**, 327, 313-5.
- (28) Aragão-Leoneti, V.; Campo, V. L.; Gomes, A. S.; Field, R. A.; Carvalho, I. *Tetrahedron* **2010**, 66, 9475-9492.
- (29) Alonso, F.; Moglie, Y.; Radivoy, G.; Yus, M. *Tetrahedron Letters* **2009**, 50, 2358-2362.
- (30) Tasdelen, M. A.; Yagci, Y. *Tetrahedron Letters* **2010**, 51, 6945-6947.
- (31) Gill, H. S.; Marik, J. *Nature protocols* **2011**, 6, 1718-25.

- (32) Nakamura, T.; Terashima, T.; Ogata, K.; Fukuzawa, S.-Ichi *Organic Letters* **2011**, *13*, 620-623.
- (33) Díez-González, S.; Escudero-Adán, E. C.; Benet-Buchholz, J.; Stevens, E. D.; Slawin, A. M. Z.; Nolan, S. P. *Dalton Transactions* **2010**, *39*, 7595-606.
- (34) Teyssot, M.-L.; Nauton, L.; Canet, J.-L.; Cisnetti, F.; Chevry, A.; Gautier, A. *European Journal of Organic Chemistry* **2010**, *2010*, 3507-03515.
- (35) Baeza, B.; Casarrubios, L.; Ramirez-Lopez, P.; Gomez-Gallego, M.; Sierra, M. A. *Organometallics* **2009**, *28*, 956-959.
- (36) Broggi, J.; Díez-González, S.; Petersen, J. L.; Berteina-Raboin, S.; Nolan, S. P.; Agrofoglio, L. A. *Synthesis-Stuttgart* **2008**, 141-148.
- (37) Díez-González, S.; Nolan, S. P.; Díez-González, S. *Synlett* **2007**, *2007*, 2158-2167.
- (38) Díez-González, S.; Stevens, E. D.; Nolan, S. P. *Chemical Communications* **2008**, 4747-4749.
- (39) Gu, S. J.; Xu, H.; Zhang, N.; Chen, W. Z. *Chemistry-an Asian Journal* **2010** *5*, 1677-1686.
- (40) Partyka, D. V.; Gao, L.; Teets, T. S.; Updegraff, J. B.; Deligonul, N.; Gray, T. G. *Organometallics* **2009**, *28*, 6171-6182.
- (41) Mobian, P.; Collin, J.-P.; Sauvage, J.-P. *Tetrahedron Letters* **2006**, *47*, 4907-4909.
- (42) Durot, S.; Mobian, P.; Collin, J.; Sauvage, J. *Tetrahedron* **2008**, *64*, 8496-8503.
- (43) Kasani, A.; Babu, R. P. K.; McDonald, R.; Cavell, R. G. *Angewandte Chemie-International Edition* **1999**, *38*, 1483-1484.
- (44) Doux, M.; Ricard, L.; Mathey, F.; Floch, P. L.; Mézailles, N. *European Journal of Inorganic Chemistry* **2003**, 687-698.
- (45) Doux, M.; Mézailles, N.; Ricard, L.; Floch, P. *Le European Journal of Inorganic Chemistry* **2003**, 3878-3894.
- (46) Doux, M.; Mézailles, N.; Melaimi, M.; Ricard, L.; Floch, P. L. *Chemical Communications* **2002**, *377*, 1566-1567.

- (47) Doux, M.; Me, N.; Ricard, L.; Floch, P. L. *Communications* **2003**, 4624-4626.
- (48) Doux, M.; Bouet, C.; Mézailles, N.; Ricard, L.; Floch, P. Le *Organometallics* **2002**, *21*, 2785–2788.
- (49) Cantat, T.; Mezailles, N.; Ricard, L.; Jean, Y.; Floch, P. Le *Angewandte Chemie-International Edition* **2004**, *43*, 6382-6385.
- (50) Lambert, C.; Ragu Schleyer, P. von *Angewandte Chemie International Edition in English* **1994**, *33*, 1129-1140.
- (51) Ritchie, J. P.; Bachrach, S. M. *Journal of the American Chemical Society* **1987**, *109*, 5909-5916.
- (52) Cavell, R. G.; Kamalesh Babu, R. P.; Aparna, K. *Journal of Organometallic Chemistry* **2001**, *617-618*, 158-169.
- (53) Kamalesh Babu, R. P.; McDonald, R.; Decker, S. a.; Klobukowski, M.; Cavell, R. G. *Organometallics* **1999**, *18*, 4226-4229.
- (54) Kamalesh Babu, R. P.; Cavell, R. G.; McDonald, R. *Chemical Communications* **2000**, *668*, 481-482.
- (55) Appel, R.; Ruppert, I. *Zeitschrift Fur Anorganische Und Allgemeine Chemie* **1974**, *406*, 131-144.
- (56) Kasani, A.; Babu, R. P. K.; Mcdonald, R.; Cavell, R. G. *Organometallics* **1999**, *2*, 1483-1484.
- (57) Ma, G.; Ferguson, M. J.; McDonald, R.; Cavell, R. G. *Organometallics* **2010**, *29*, 4251-4264.
- (58) The, D.; Kitagawa, S.; Munakata, M. *Inorganic Chemistry* **1981**, *20*, 2261-2267.
- (59) Kitagawa, S.; Munakata, M.; Miyaji, N.; October, R. *Inorganic Chemistry; Section E* **1982**, *21*, 3842–3843.
- (60) Baird, W. C.; The, T. O. *Journal of the American Chemical Society* **1963**, *85*, 1009-1010.
- (61) Leedham, T. J.; Powell, D. B.; Scott, J. G. V. *Spectrochimica Acta Part A: Molecular Spectroscopy* **1973**, *29*, 559-565.

- (62) Jones, N. D.; Lin, G.; Gossage, R. A.; McDonald, R.; Cavell, R. G. *Organometallics* **2003**, *22*, 2832–2841.
- (63) Jones, N. D.; Cavell, R. G. *Journal of Organometallic Chemistry* **2005**, *690*, 5485-5496.
- (64) Klobukowski, M.; Decker, S. A.; Lovallo, C. C.; Cavell, R. G. *Journal of Molecular Structure: THEOCHEM* **2001**, *536*, 189-194.
- (65) Sandor, M.; Geistmann, F.; Schuster, M. *Analytica Chimica Acta* **2003**, *486*, 11-19.
- (66) Kunkely, H.; Vogler, A. *Inorganic Chemistry Communications* **2006**, *9*, 1-3.
- (67) Holzner, C.; Goesmann, K. K. H. *Monatshefte* **1994**, *125*, 1339-1352.
- (68) Holzner, C. *Monatshefte* **1994**, *125*, 1353-1364.
- (69) Wang, X.-yong; Guerzo, A. Del; Schmehl, R. H. *Journal of Photochemistry and Photobiology C: Photochemistry Reviews* **2004**, *5*, 55-77.
- (70) Ford, P. C.; Vogler, A. *Accounts of Chemical Research* **1993**, *26*, 220-226.
- (71) Vogler, A.; Kunkely, H. *Journal of the American Chemical Society* **1986**, *108*, 7211-7212.
- (72) Sabin, F.; Ryu, C. K.; Ford, P. C.; Vogler, a. *Inorganic Chemistry* **1992**, *31*, 1941-1945.
- (73) Kok, J. M.; Skelton, B. W.; White, A. H. *Journal of Cluster Science* **2004**, *15*, 365-376.
- (74) Teo, B.-K.; Calabrese, J. C. *Inorganic Chemistry* **1976**, *15*, 2467-2474.
- (75) Ichinaga, A. K.; Kirchoff, J. R.; McMillin, D. R.; Dietrich-Buchecker, C. O.; Marnot, P. A.; Sauvage, J. P. *Inorganic Chemistry* **1987**, *26*, 4290–4292.
- (76) Kyle, K. R.; Palke, W. E.; Ford, P. C.; Kyle, R.; Palke, E.; Ford, C. *Coordination Chemistry Reviews* **1990**, *97*, 35-46.
- (77) Wing-Wah Yam, V.; Kam-Wing Lo, K.; Kit-Mai Fung, W.; Wang, C.-R. *Coordination Chemistry Reviews* **1998**, *171*, 17-41.

- (78) Jutand, A. *Chemical reviews* **2008**, *108*, 2300-47.
- (79) Aparna, K.; McDonald, R.; Ferguson, M.; Cavell, R. G. *Organometallics* **1999**, *18*, 4241-4243.
- (80) Cavell, R.; Aparna, K.; Kamalesh Babu, R. P.; Wang, Q. *Journal of Molecular Catalysis A: Chemical* **2002**, *189*, 137-143.
- (81) Heinze, J. *Angewandte Chemie International Edition in English* **1984**, *23*, 831-847.
- (82) Faulkner, L. R.; Bard, A. J. *Electrochemical Methods: Fundamentals and Applications (2ed.)*; Wiley, **1980**, 1-718.

Chapter 3:

The Formation of a

Tri-lithium

Bis(iminodiphenylphosphorano)

methanide

Copper (I) Dichloride

Complex

3.1 Introduction

3.1.1 Catalytic Properties

Changing one or two atoms within a molecule can substantially alter the properties (i.e., optical response, reactivity, etc.). The Goldman and Brookhart groups have shown exchanging carbon for oxygen changes catalytic cycles. In Figure 3.1, the structures of three iridium pincer compounds that are used in the catalytic dehydrogenation of alkanes to alkenes are depicted. **A** and **B** only differ in alkyl substituents bound to the phosphorus atoms, which provide differing degrees of steric crowding around the metal centre. The additional steric bulk limits the ability of the alkanes to access the metal centre, which is a vital step in the process of catalytic dehydrogenation. Catalyst **A** shows higher turn over numbers than **B** for C-H insertion reactions, both catalysts show similar regioselectivity.

In catalyst **C**, the two methylene carbons have been replaced by oxygen atoms, resulting in an electronic influence around the metal centre. The result was a change in the regioselectivity of the catalytic process, wherein **C** can form terminal as well as the common internal alkenes due to better accessibility to the iridium metal centre.¹⁻⁶

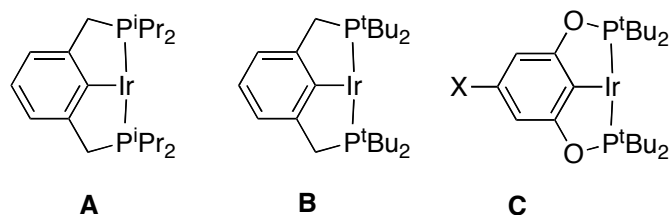


Figure 3.1: Iridium pincer complexes. a) (*i*Pr₄-PCP)Ir, b) (*t*Bu₄-PCP)Ir and c) (*t*Bu₄-POCOP)Ir, for the use as catalysts in the formation of terminal alkenes, (adapted from reference 2)²

3.1.2 Optical Properties

In addition to the copper complex discussed in Chapter 2 that acted as a copper (II) sensor, a variety of copper complexes whose photoluminescent maximum is in the visible region of the electromagnetic spectrum have been prepared. In a recent publication from the Pike group, with the goal of developing a copper-based amine sensor, a variety of copper (I) cyanide compounds with amine or sulfide ligands were synthesized. Twenty-nine compounds of varied composition were prepared, and found to have luminescence ranging from blue to red in the visible spectrum under UV irradiation, which depended heavily upon the particular substituent ligand.⁷⁻¹⁰

Figure 3.2 below is a representation of two compounds form by the Pike group and the range of colours observed in the complete set.⁷

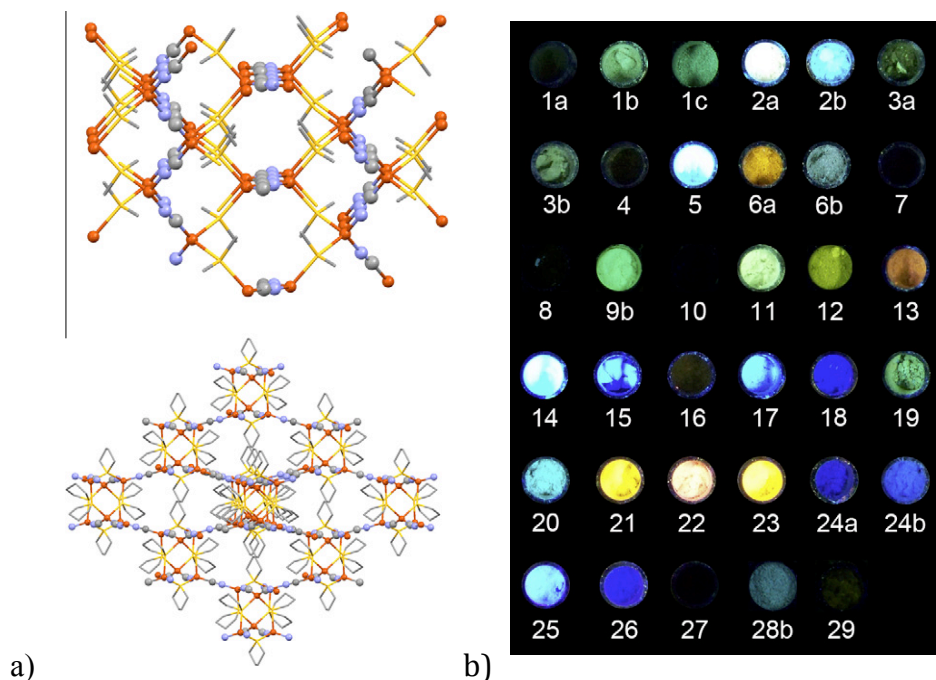
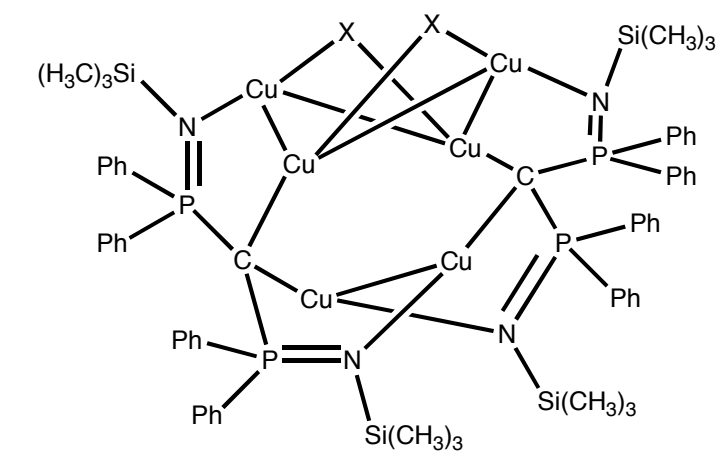


Figure 3.2: Schematic representation of the X-ray structures, a) top: $(\text{CuCN})_3(\text{Me}_2\text{S})$, bottom $(\text{CuCN})(\text{THT})$. (THT = tetrahydrothiophene), b) $(\text{CuCN})L_n$ irradiated at 254 and 365nm; the polymers represented in a) are represented as 28b and 29⁷

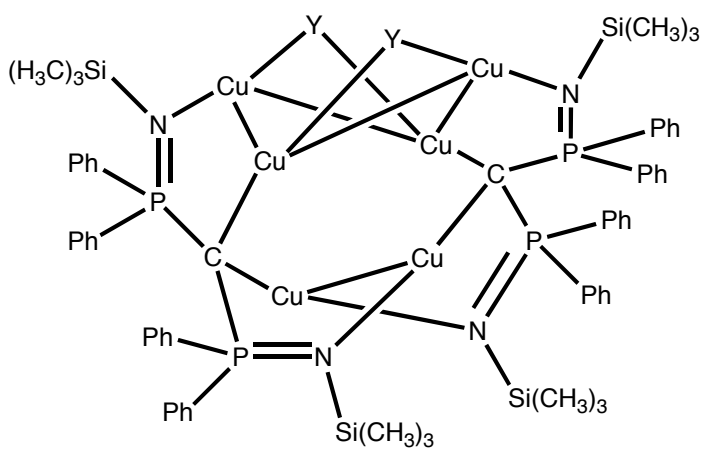
3.1.3 The Original Goal: Copper as a Sensor and/or Catalyst

We were interested in investigating how changing the coordination environment around the copper (I) centre would impact the properties of the cluster and pincer complexes. In this context, we chose to vary the auxiliary ligands in the copper clusters described in Chapter 2 by exchanging the halide caps with chalcogenide-based ligands (Scheme 3.1).



X = Cl, Br, I

Chalcogenide precursor
 Y = O, S, Se-based ligands
 Solvent = THF, Ether



Scheme 3.1: Capping ligand, X, exchanged with a chalcogenide-based precursor, Y, to form a new cluster with Y at the caps

Each newly synthesized complex would be characterized by spectroscopic methods (i.e. NMR, mass spectroscopy, etc.) as well as through X-ray crystallography and any corresponding changes in the optical and/or electronic properties would be measured, in order to understand the versatility of copper as a potential sensor or as a catalyst.

3.2 Experimental

3.2.1 Materials:

All materials were purchased from Sigma-Aldrich and used as received unless otherwise specified. Azido trimethylsilane, bis(diphenylphosphino)methane, 2,2'-bipyridine, copper (I) chloride, tri-phenyl phosphine, thiophenol ($\geq 99\%$), and 1.4M *n*-butyl lithium in diethyl ether were purchased from Sigma-Aldrich and used as received. Tetrahydrofuran (THF) and toluene were dried over and distilled from sodium/benzonphenone ketyl, diethyl ether (Et₂O) was obtained from an Innovative Technology Inc. PureSolv solvent system and acetonitrile was distilled from calcium hydride.

3.2.2 General Methods:

All manipulations were performed in anaerobic environments using strict Schlenk techniques or an argon-filled mBraun glove box. NMR spectra (¹H, ¹³C, and ³¹P) were obtained using a Varian I400 spectrometer operating at frequencies of 400, 100, and 162 MHz, respectively. Referencing for the ¹H and ¹³C NMR spectra was done using residual solvent protons and solvent resonances,

respectively. Chemical shifts for all ^{31}P NMR spectra were referenced to an 85% H_3PO_4 external solution. All NMR data was reported in parts per million (ppm) and J coupling constants are reported in Hertz (Hz). Abbreviations for the NMR data include: s: singlet, d: doublet, t: triplet, and m: multiplet. Crystallographic data was collected using graphite-monochromated Mo $\text{K}\alpha$ radiation (0.71073 Å) on a Bruker D8/APEX II CCD Diffractometer

3.2.3 Synthetic Procedure:

Synthesis of $\{[(\text{C}_4\text{H}_8\text{O})_4\text{Li}_3(\text{CH}(\text{Ph}_2\text{P}=\text{N})_2)_2]^+[\text{CuCl}_2]^- \}$ (**6**)

In the glovebox, a solution was prepared by mixing solid $[\text{Li}_2\text{C}(\text{Ph}_2\text{P}=\text{NSiMe}_3)_2]$ and $\text{Cu}_2\text{Cl}_2(\text{cod})_2$ complexes in 1:3 molar ratio in THF. The presence of the intermediate, $[\text{Cu}_6\{\text{C}(\text{Ph}_2\text{P}=\text{NSiMe}_3)_2\}_2\text{Cl}_2]$, was confirmed by ^{31}P NMR spectroscopy. To this solution, excess thiophenol was added and the reaction mixture was stirred at room temperature for 24 hours. A yellow-green precipitate formed and was removed via centrifugation. The remaining clear yellow solution was isolated and solvent was removed, using a vacuum line housed within the glovebox, to a point of saturation (i.e., the solution became cloudy). Suitable yellow crystals were obtained after allowing the solution to stand undisturbed for a few days at room temperature.

Representative synthesis for halide exchange with chalcogenide-based compounds

In the glovebox, a solution was prepared by mixing solid or solution-based (**1**), (**2**), or (**3**) and a chalcogenide-based complex (see Table 3.1 for the list of combinations) in varying molar ratios (i.e., 1:3 or 1:10) in either THF or diethyl ether. The reaction mixture was stirred at room temperature between 1-24 hr, carefully monitoring the reaction mixture for any changes. Aliquots were taken of the samples periodically to run ^{31}P NMR spectroscopy in order to evaluate the extent of reaction. If the solution was deemed to be complete via NMR, the solution was isolated and solvent was removed, using a vacuum line housed within the glovebox, to a point of saturation (i.e., the solution became cloudy). Crystal growth was then attempted by allowing the solution to stand undisturbed for a few days at room temperature. If X-ray crystallographic quality crystal were achieved, structure confirmation was attempted.

3.3 Results and Discussion

The halide ligands were targeted for the facile exchange through the formation of a halide salt. The exchange of the hexanuclear copper complex halide ligands was first attempted using oxo- and thio-based ligands with extension towards trying selenium-based ligands. The goal of preparing these complexes was to investigate how their photoluminescence response would be altered through this change in the coordinative environment of the Cu centre. Previously we determined that changing the halide had little influence on the complex photoluminescent response. The three halide-based hexanuclear copper

clusters remained an orange-red colour under UV irradiation despite the caps varying, from Cl⁻ to I⁻. It was expected that the exchange with chalcogenides at the caps sites would be analogous to the halides, in that the luminescence properties should remain consistent. It was shown recently, by the Cavell group, that the exchange of chloride, in a hexanuclear copper cluster, with potassium tertiary-butyl oxide could be done to completion, as shown by ³¹P NMR analysis. The compound, represented in Figure 3.3 has a green luminescence under UV-light.¹¹

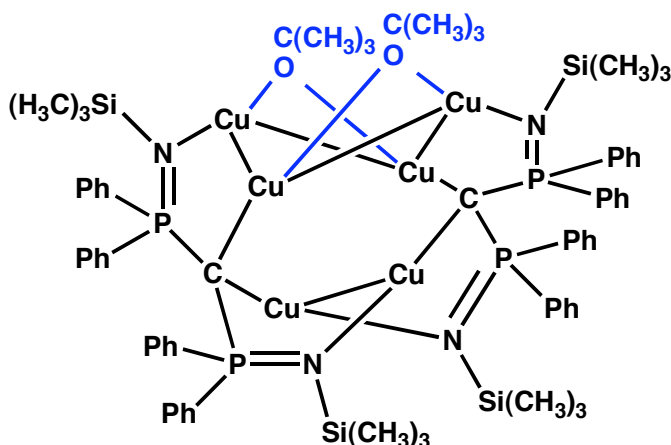


Figure 3.3: Chalcogenide-based hexanuclear copper cluster: $[Cu_6L_2(O^tC(CH_3)_3)_2]$, where $L = C(Ph_2P=NSiMe_3)_2^{2-}$, (adapted from reference)¹¹

Formation of hexanuclear copper clusters, discussed in Chapter 2 (i.e. compound **3**, **4** and **5**), was the starting point for the present exchange reactions. Replacement of the halide caps by chalcogenide-based ligands was attempted. Represented in Table 3.1 are the reactions attempted in order to exchange the halide caps with a chalcogenide-based ligand.

Table 3.1 Formation of hexanuclear copper clusters with various chalcogenide caps

<i>Reagent 1</i>	<i>Reagent 2</i>	<i>Solvent</i>	<i>Reaction (yes/no)</i>	<i>Luminescence (colour)</i>
3	<i>NaHSe</i>	<i>Et₂O</i>	<i>No</i>	<i>Orange</i>
3	<i>NaHS</i>	<i>Et₂O</i>	<i>No</i>	<i>Orange</i>
3, 4, 5	<i>KOC(CH₃)₃</i>	<i>Et₂O/THF</i>	<i>Yes</i>	<i>Light Green</i>
3	<i>S₈</i>	<i>Et₂O</i>	<i>No</i>	<i>Not Observed</i>
3	<i>Se</i>	<i>Et₂O</i>	<i>No</i>	<i>Orange</i>
3	<i>NaOCH₃</i>	<i>Methanol/Et₂O</i>	<i>No</i>	<i>Not Observed</i>
3	<i>LiOCH(CH₃)₂</i>	<i>THF</i>	<i>Yes</i>	<i>Light Green</i>
4	<i>SH(CH₂)₃CH₃</i>	<i>THF</i>	<i>Yes^h</i>	<i>Green</i>
3	<i>Na₂S</i>	<i>Et₂O</i>	<i>Yes</i>	<i>Yellow</i>
4	<i>(C₆H₅)SeCl</i>	<i>THF</i>	<i>No</i>	<i>Not Observed</i>
4	<i>(C₆H₅)₂Se₂</i>	<i>THF</i>	<i>No</i>	<i>Not Observed</i>
3,4	<i>(C₆H₅)SH</i>	<i>THF</i>	<i>No</i>	<i>Not Observed</i>
2	<i>Cu₂O</i>	<i>Et₂O/THF</i>	<i>No</i>	<i>Not Observed</i>
2	<i>Cu₂Se</i>	<i>Et₂O</i>	<i>No</i>	<i>Not Observed</i>
2	<i>CuBrS(CH₃)₂</i>	<i>Benzene (d₆)</i>	<i>No</i>	<i>Not Observed</i>
1	<i>CuBrS(CH₃)₂</i>	<i>THF</i>	<i>No</i>	<i>Not Observed</i>

h Crystal structure obtained for $\{[(C_4H_8O)_4Li_3(CH(Ph_2P=N)_2)_2]^+ [CuCl_2]^- \}$

Unfortunately, in most cases, only starting material or complex product mixtures were obtained. It is worth noting that, some complex product mixtures displayed green luminescence upon exposure to UV light (refer to Table 3.1). This observation is consistent with other reports of complexes with chalcogenides to copper, however without conclusive characterization no definitive statements regarding the identity of these complexes can be made. In this regard, the following discussion only describes the case where a crystal structure of the product was obtained even though it does not contain a targeted hexanuclear copper cluster structural motif.

The formation of $\{[(C_4H_8O)_4Li_3(CH(Ph_2P=N)_2)_2]^+[CuCl_2]^{-}\}$, herein known as compound **6**, was achieved by mixing **3**, dissolved in THF, with the precursor of choice (e.g., thiophenol) until no precipitation was observed. After the reaction was completed and the product-containing solution was isolated, a crystal suitable for X-ray diffraction analysis was isolated. From the X-ray structure (Figure 3.4) it was determined that the original cluster (i.e., **3**) had broken apart to form the unique lithium-trimeric compound consisting of lithium atoms surrounded by two bis(diphenyltrimethylsilyliminophosphorano)methanide ligand structures, shown in Figure 3.5. The original six copper atom cluster was not present in the crystallized product. Throughout the reactions, the copper and chloride atoms come within close proximity to form the counter-ion, $[CuCl_2]^{-}$. The complex was determined by structural analysis to have four THF solvent molecules, eight in each unit cell.

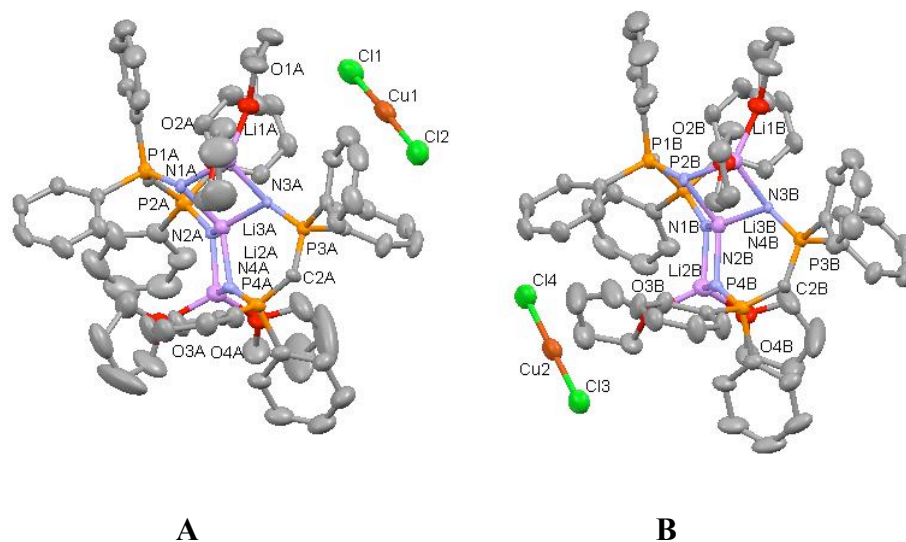


Figure 3.4: Calculated crystal structure of $\{(C_4H_8O)_4Li_3(CH(Ph_2P=N)_2)_2\}^+[CuCl_2]^-$, two complexes comprise the unit cell denoted as *A* (left complex) and *B* (right complex)

The three lithium atoms act as a bridge between the two orthogonal ligands; the lithiated complex forms a cation with a linear $[Cl-Cu-Cl]^-$ counter anion.

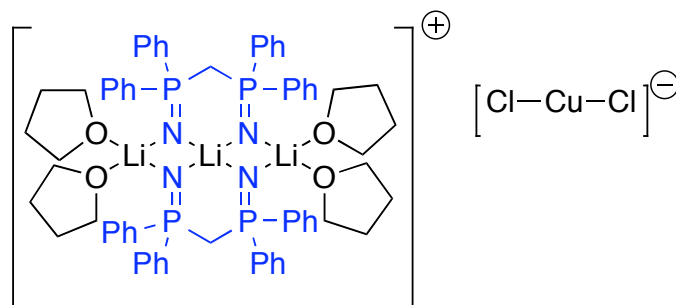
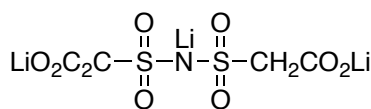


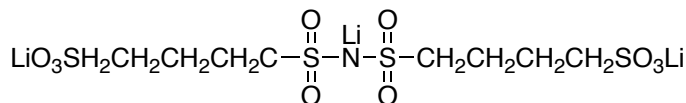
Figure 3.5: Tri-lithium bis(iminodiphenylphosphorano)methanide copper (I) dichloride

Compound **6** is, to the best of our knowledge, the first example of a directly bridged lithium system. Most of the salts studied to date do not have bridged lithium atoms; they have lithium atoms bonded to nitrogen atoms. Tri-

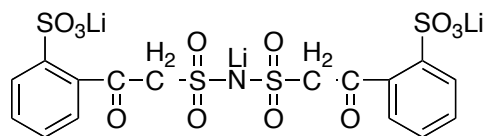
lithium salts with Li-N moieties are known to exhibit good electrochemical stability and have potential uses in lithium ion batteries. While mono-lithiated species are employed in batteries,¹² tri-lithiated salts offer the added benefit of being more cost effective and more environmentally friendly, because of higher atom economy, and more lithium atoms available for energy producing reactions. In the examples shown below (Figure 3.6) the lithium atoms have a separation range of three up to six atoms between.



TLS-1



TLS-2



TLS-3

Figure 3.6: Tri-lithiated salts for battery applications. TLS-1, [N-lithium bis(carboxylithium methanesulfon)imide]; TLS-2, [N-lithium bis(4-lithiumsulfonatobutane)sulfonimide]; TLS-3, [N-lithium bis(o-lithiumsulfonatoacetophenonyl)sulfonimide]¹²

The unit cell contains two $[(\text{C}_4\text{H}_8\text{O})_4\text{Li}_3(\text{CH}(\text{Ph}_2\text{P}=\text{N}))_2]^+[\text{CuCl}_2]^-$ molecules, labeled A and B (Figure 3.4) in a monoclinic lattice with eight THF molecules. The two molecules are unique in that slight differences in bond angles as well as bond distances were observed through the X-ray crystallographic

analysis. The bis(diphenyltrimethylsilyliminophosphorano)methanide ligand shows P-C-P bond angles extended to 130.1(2)°/125.5(2)° and 128.2(2)°/127.4(2)° for structures A and B respectively, which are comparable to the previously synthesized doubly-deprotonated **2**, (132.4(3)°), mono-deprotonated structures such as $[\text{Na}\{\mu^2\text{-CH}(\text{R}_2\text{P}=\text{NSiMe}_3)_2\text{-}\kappa^3\text{N,N,N'}\}]_2$, as well as those that have been chelated with various metals; angles vary between 127-134°. ^{13,14} The P-C bonds and P-N bonds, which were calculated to range from 1.568(2) Å – 1.596(2) Å and from 1.503(2) Å - 1.525(2) Å, respectively, formed the 6-membered ring structure by shortening and lengthening appropriately to accommodate the ring completion and closure. The two six-membered rings mentioned are comprised of lithium, two nitrogens, two phosphorus and a methanide carbon. The electron density expressed by the two methanide carbons is balanced by the positively-charged lithium atoms, which increases overall stability. ¹⁴⁻¹⁸

The Li-N bond distances were found to be between 1.918(5) Å and 1.9601(5) Å. These distances are shorter than other literature reported distances which can be up to 2.152(9) Å, but are still within the range of single bond character as was seen in previous work which observed Li-N distances within 1.997(9) Å–2.050(9) Å. ^{19,20} The polymeric $(\text{Li}_4\text{Am}_3)^+ \cdot \{\text{Li}[(\mu\text{-Me})_2\text{Al}(\text{Me})t\text{Bu}]_2\}^-$, has many similar characteristics to the structure being described. ²¹ The key features includes, a ring system with bond distances between 1.992(6) – 2.016(6) Å and a section of Li-N bond distances between 2.064(7) – 2.199(6) Å with regard to bond distances connecting lithium atoms to the ring systems reported are

comparable to **6**. The Li-N bond lengths and angles were also consistent with other literature reports of structure wherein lithium atoms were used to bridge metal-based compounds to form cluster species.^{21–24}

Chromium (II) organochromate complexes were determined, by Gambarotta *et al.*, to have Li-N-Li bond angles on the order of 84.5(4)° and Li-N bond lengths averaging slightly longer than those of compound **6** at a range of 2.06(1)-2.15(1) Å; however, the longer lengths can be attributed to twisted nature of the chromium species as a whole, seen below in Figure 3.7.²⁵

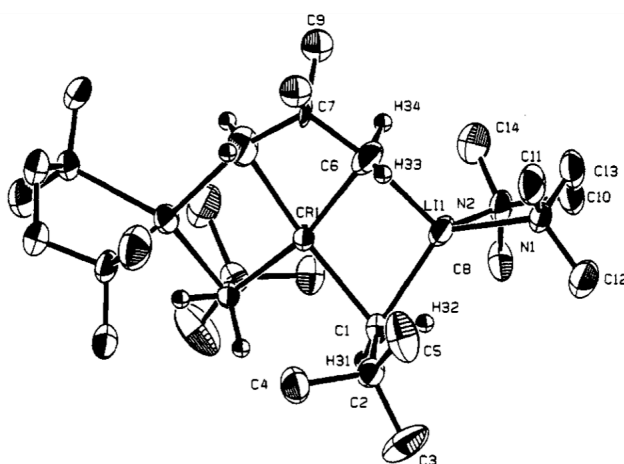


Figure 3.7: ORTEP of $[(\text{CH}_3)_3\text{CCH}_2]_2[\text{CH}_2\text{C}(\text{CH}_3)_2\text{CH}_2]\text{-Cr}[\text{Li}(\text{TMEDA})]_2$. Thermal ellipsoids were drawn at 50% the probability level²⁵

The counter ion in the structure below is a monoanionic $[\text{CuCl}_2]^-$ where in the copper atom remains as a stable entity in the +1 oxidation state as opposed to being oxidized to a Cu^{+2} state. The structure, shown in Figure 3.4, has a nearly linear (178.61°, 178.29°) Cl-Cu-Cl structure with Cu-Cl bond distances of 2.0979(11) Å and 2.1016(12) Å, for the molecule denoted as A, 2.1094(10) Å and

2.1100(11) Å, for the molecule denoted as B; these are comparable to values reported in the literature of dichlorocuprate (I) structures.²⁶⁻³¹

3.4 Conclusions

A unique tri-lithium complex where the lithium atoms are directly bonded to one another was serendipitously discovered. Most tri-lithiated compounds do not have lithium atoms in such proximity to one another unless in clusters of two. The resulting tri-lithium bis(iminodiphenylphosphorano)methylene copper (I) dichloride also illustrates that, despite the hexanuclear copper cluster being broken apart, the backbone can still hold together a cluster formation through bilateral binding.

3.5 References

- (1) Ahuja, R.; Punji, B.; Findlater, M.; Supplee, C.; Schinski, W.; Brookhart, M.; Goldman, A. S. *Nature chemistry* **2011**, *3*, 167-71.
- (2) Choi, J.; MacArthur, A. H. R.; Brookhart, M.; Goldman, A. S. *Chemical reviews* **2011**, *111*, 1761-79.
- (3) Findlater, M.; Cartwright-Sykes, A.; White, P. S.; Schauer, C. K.; Brookhart, M. *Journal of the American Chemical Society* **2011**, *133*, 12274-84.
- (4) Punji, B.; Emge, T. J.; Goldman, A. S. *Organometallics* **2010**, *29*, 2702-2709.
- (5) Ray, A.; Kissin, Y. V.; Zhu, K.; Goldman, A. S.; Cherian, A. E.; Coates, G. W. *Journal of Molecular Catalysis A: Chemical* **2006**, *256*, 200-207.
- (6) Zhang, X.; Wang, D. Y.; Emge, T. J.; Goldman, A. S. *Inorganica Chimica Acta* **2011**, *369*, 253-259.
- (7) Dembo, M. D.; Dunaway, L. E.; Jones, J. S.; Lepekhina, E. A.; McCullough, S. M.; Ming, J. L.; Li, X.; Baril-Robert, F.; Patterson, H. H.; Bayse, C. A. *Inorganica Chimica Acta* **2010**, *364*, 102-114.
- (8) Bayse, C. A.; Ming, J. L.; Miller, K. M.; McCollough, S. M.; Pike, R. D. *Inorganica Chimica Acta* **2011**, *375*, 47-52.
- (9) Pike, R. D.; deKrafft, K. E.; Ley, A. N.; Tronic, T. a *Chemical Communications (Cambridge, England)* **2007**, *20*, 3732-4.
- (10) Tronic, T. a; deKrafft, K. E.; Lim, M. J.; Ley, A. N.; Pike, R. D. *Inorganic Chemistry* **2007**, *46*, 8897-912.
- (11) Ma, G.; Ferguson, M. J.; McDonald, R.; Cavell, R. G. *Organometallics* **2010**, *29*, 4251-4264.
- (12) Luo, K.; Filler, R.; Mandal, B. *Solid State Ionics* **2006**, *177*, 857-861.
- (13) Kamalesh Babu, R. P.; Aparna, K.; McDonald, R.; Cavell, R. G. *Organometallics* **2001**, *20*, 1451-1455.
- (14) Kasani, A.; Babu, R. P. K.; McDonald, R.; Cavell, R. G. *Angewandte Chemie-International Edition* **1999**, *38*, 1483-1484.

- (15) Ma, G. B.; McDonald, R.; Cavell, R. G. *Organometallics* **2009**, *29*, 52-60.
- (16) Kasani, A.; Babu, R. P. K.; McDonald, R.; Cavell, R. G. *Organometallics* **1999**, *2*, 1483-1484.
- (17) Wooles, A. J.; Cooper, O. J.; McMaster, J.; Lewis, W.; Blake, A. J.; Liddle, S. T. *Organometallics* **2010**, *29*, 2315-2321.
- (18) Kamalesh Babu, R. P.; McDonald, R.; Cavell, R. G.; Babu, R. P. K. *Organometallics* **2000**, *19*, 3462-3465.
- (19) Hatipoğlu, A.; Selçuki, C.; Aviyente, V.; Cinar, Z.; Hatipoglu, A.; Selcuki, C. *Journal of Molecular Modeling* **2002**, *8*, 156-167.
- (20) Kamalesh Babu, R. P.; Aparna, K.; McDonald, R.; Cavell, R. G. *Inorganic Chemistry* **2000**, *39*, 4981-4984.
- (21) Davies, R. P. P.; Linton, D. J. J.; Schooler, P.; Snaith, R.; Wheatley, A. E. E. H. H. *European Journal of Inorganic Chemistry* **2001**, *2001*, 619-622.
- (22) Karsch, H. H.; Schreiber, K.-A.; Reisky, M. *Organometallics* **1999**, *18*, 3944-3946.
- (23) Armstrong, D.; Clegg, W.; Davies, R. *Angewandte Chemie International Edition* **1999**, *38*, 3367-3370.
- (24) Armstrong, D. R.; Khandelwal, A. H.; Raithby, P. R.; Kerr, L. C.; Peasey, S.; Shields, G. P.; Snaith, R.; Wright, D. S. *Chemical Communications* **1998**, *2*, 1011-1012.
- (25) Hao, S.; Song, J. I.; Berno, P.; Gambarotta, S. *Organometallics* **1994**, *13*, 1326-1335.
- (26) Healy, P. C.; Kildea, J. D.; Skelton, B. W.; White, A. H. *Australian Journal of Chemistry* **1989**, *42*, 115-136.
- (27) Rodenstein, A.; Creutzburg, D.; Schmiedel, P.; Griebel, J.; Hennig, L.; Kirmse, R. *Zeitschrift Fur Anorganische Und Allgemeine Chemie* **2008**, *634*, 2811-2818.
- (28) Wang, J.-G.; Kang, H.-X.; Zheng, X.-Y. *Zeitschrift für Kristallographie. New crystal structures* **2005**, *220*, 597-598.
- (29) Mirkhani, V.; Harkema, S.; Kia, R. *Acta Crystallographica Section C- Crystal Structure Communications* **2004**, *60*, M343-M344.

- (30) Zheng, Y.-Z.; Ng, S. W. *Acta Crystallographica Section E Structure Reports Online* **2005**, *61*, 1030-1032.
- (31) Healy, P. C.; McMurtrie, J. C.; Bouzaid, J. *Acta crystallographica. Section E, Structure reports online* **2010**, *66*, 493-4.

Chapter 4:

Conclusions

And

Future Work

4.1 Conclusions

This thesis has described the evolution from the first introduction of C^{-2} , through the formation of carbenes finally describing the synthesis of a hexanuclear copper cluster. The goal was to demonstrate the versatility of copper as an element under various reaction conditions and demonstrate copper complexes as viable compounds for sensor and catalytic activity.

Chapter 2 demonstrated the formation of a hexanuclear copper cluster with luminescent properties. The electrochemical redox properties were evaluated using cyclic voltammetry. The results for each of the halide-based hexanuclear copper clusters indicated a stripping peak during the reductive cycle of the cyclic voltammogram, as copper is plated on the electrode then subsequently removed via electronically stripping the base. It was found that oxidation of the clusters was not reversible in all cases. The redox activity of each cluster indicated that more work needs to be done on structure development if the clusters are to be used as catalysts.

To explore the luminescent properties of the hexanuclear copper clusters, reactions in which the halide caps were exchanged with various chalcogenide precursors to place a new ligand in the cap locations of the clusters. The premise was a new electronic environment could afford green luminescence. The attempted exchange reactions gave a new unique complex. Unfortunately, straight-forward ligand exchange did not occur and the original cluster was broken apart forming a tri-lithiated complex with a copper chloride counter-anion.

The new complex has potential in lithium ion battery applications; however, further research is required if practical applications are to be realized.

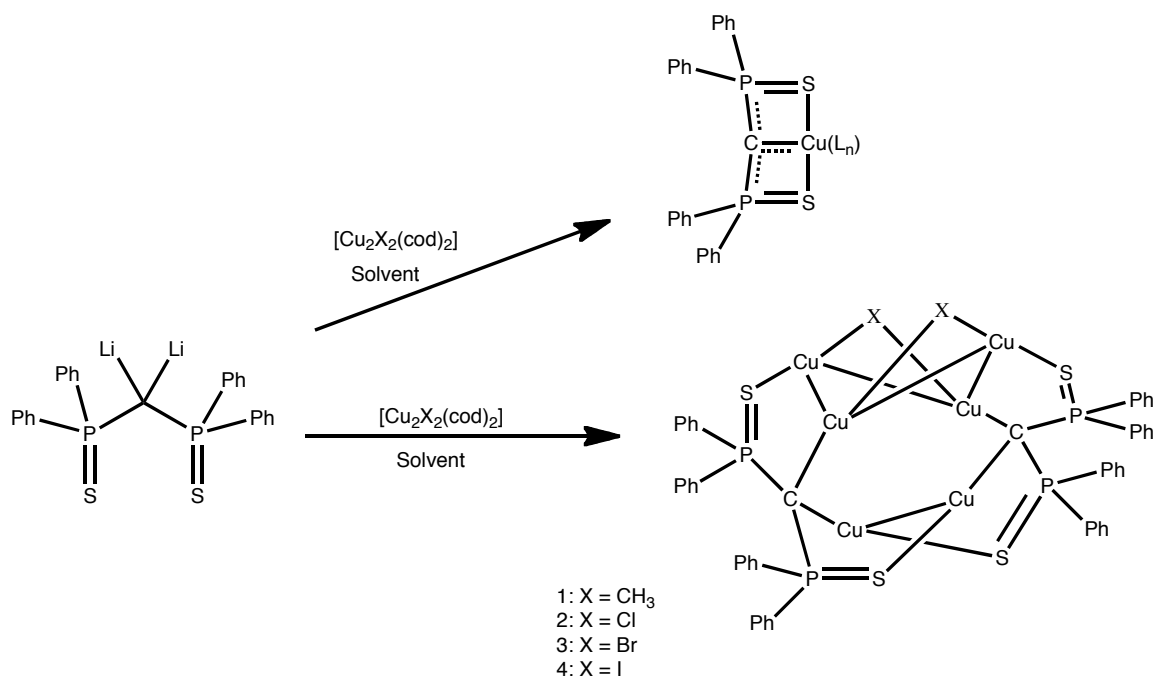
4.2 Future Work

In addition to the examples shown in Table 3.1, a rational approach to continuing this work would involve methodically evaluating the role of the solvent and other reaction conditions, such as: reaction times, solvent ratios and combinations and assisting reagents. The goal of these future investigations would be to force complete precipitation of the halide salt from the hexanuclear copper clusters to yield a new hexanuclear copper cluster with chalcogenide-based ligands as the capping agents. If initial characterization showed the formation of the desired products, a comprehensive evaluation of the luminescent and electronic properties would be key in developing prospective applications for each complex. In addition to attempting to obtain crystals to confirm the bonding domains it would also be beneficial to run low temperature NMR to explore the mechanism by which the exchange at the cluster caps occurs.

NMR and other spectroscopic studies may also shed light onto the formation of the tri-lithiated complex with regard to the formation of any side products and the deformation of the hexanuclear copper cluster. As was found upon analysis of the crystal structure of the tri-lithiated complex, the cluster broke apart and re-formed into the above-mentioned complex; however, analysis of the side-products was not achieved (see Chapter 3).

Upon complete formation of any of the halide or chalcogenide-based hexanuclear copper clusters an evaluation into possible applications would be of value. Initial thoughts for the clusters would be as catalysts for olefin polymerization or for click chemistry. This could be achieved through the top of the cluster at the cap position; the potential steric implications could impact regioselectivity of the incoming olefin or allow two compounds to come within close proximity to undergo shifts and eliminations in order to form a desired product. Another route of activity for the clusters could be as a sensor. As the ligand preference at the cap position is dictated through bond strength and can be readily exchanged, causing shifts in the observed luminescence, the clusters could be used to sense various compounds that can act as ligands.

Unfortunately, challenges associated with the general salt metathesis method to exchange the halide caps on the hexanuclear copper clusters with chalcogenide-based ligands prevented synthesis of the desired products. It may be useful to explore alternative approaches to introducing chalcogenides into the Cu coordination sphere. Le Floch *et al.* utilize a bis(diphenylthiophosphinoyl)methane ligand as the backbone for their complexes.¹ Scheme 4.1 illustrates a potential reaction scheme in which thiolate pincer ligands afford a new bonding environment, different from that investigated here, which could yield Cu complexes with intriguing properties.



Scheme 4.1: Proposed reactions using bis(diphenylthiophosphinoyl)methaniide

Formation of the hexanuclear copper clusters using a sulfur-based ligand may introduce a new series of interactions in the realm of photo-luminescence and electronic influences without the complications of incomplete salt metathesis reactions.

Alternatively, a ligand system wherein one of the nitrogen atoms on (2) is replaced with a sulfur atom could also be attempted. Should a complex reminiscent of the top copper complex in Scheme 4.1, however, with one nitrogen and one sulfur, be synthesized the approach could give rise to a system, which could selectively coordinate compounds due to electronic interactions through the ligand. Allowing for a complex similar to that of a pincer with a dangling arm, the electronically favourable arm could be bonded to the copper when required; however, the arm would also have the flexibility of detachment upon oxidative

addition of a substrate.² Further to the research discussed in this section is the desire to expand the realm of copper complexes in order to formulate inexpensive and versatile compounds with practical applications.

4.3 References

- (1) Cantat, T.; Mezailles, N.; Ricard, L.; Jean, Y.; Le Floch, P. *Angewandte Chemie-International Edition* **2004**, *43*, 6382-6385.
- (2) Jung, B.; Hoveyda, A. H. *Journal of the American Chemical Society* **2012**, 1-4.

Appendix A1:

Crystal Structure

Determination

A1: Crystal Structure Determination

A crystal, of suitable quality, was mounted on a glass fiber by means of mineral oil; the data was collected using a graphite-monochromated Mo K α radiation (0.71073 Å) on a Bruker D8/APEX II CCD Diffractometer. The structure was solved via direct methods using SHELXL-97 and refined using full-matrix least squares F² (SHELXL-97). All non-hydrogen atoms in the structure were refined by applying anisotropic displacement parameters.

Crystal Data: $\{[(C_4H_8O)_4Li_3(CH(Ph_2P=N)_2)]^+[CuCl_2]^{-}\}$

C₆₆H₇₄Cl₂CuLi₃N₄O₄P₄

M_r = 1266.43

Monoclinic, P 2₁/C

a = 17.4946 (5) Å

b = 33.9616 (10) Å

c = 22.8825 (7) Å

α = 90.00°

β = 106.8241 (4)°

γ = 90.00°

V = 13013.6 (6) Å³

Z = 8

Mo K α radiation

μ = 0.565 mm⁻¹

T = 173 (2)

0.61 x 0.17 x 0.14 mm

Data collection:

Bruker D8/APEX II CCD diffractometer

Absorption correction: multi-scan

(SADABS; Bruker, 2002)

T_{min} = 0.7239, T_{max} = 0.9261

115399 measured reflections

29958 independent reflections

21153 reflections with I > 2 (I)

R_{int} = 0.0421

Refinement:

R[F 2 > 2 (F 2)] = 0.0552

wR(F 2) = 0.1841

S = 1.029

29958 reflections

1513 parameters

0 restraints

H-atoms treated by a mixture of independent and constrained refinement

max = 1.001 e Å³

min = -0.818 e Å³

Absolute structure: Flack (1983), 2234 Friedel pairs

Table A1.1: Selected bond lengths (Å): Structure A

N(1A)	Li(3A)	1.927(5)	N(1A)	Li(1A)	1.960(5)
N(2A)	Li(3A)	1.922(5)	N(3A)	Li(1A)	1.918(5)
N(3A)	Li(3A)	1.923(5)	N(2A)	Li(2A)	1.918(5)
N(4A)	Li(3A)	1.945(5)	N(4A)	Li(2A)	1.946(5)
O(1A)	Li(1A)	1.935(5)	O(3A)	Li(2A)	1.962(6)
O(2A)	Li(1A)	1.942(5)	O(4A)	Li(2A)	1.941(6)

Symmetry codes: (i) x, y, z; (ii) -x, y+1/2, -z+1/2; (iii) -x, -y, -z; (iv) x, -y-1/2, z-

1/2

Table A1.2: Selected bond lengths (Å): Structure B

N(1B)	Li(3B)	1.946(5)	N(1B)	Li(1B)	1.944(5)
N(2B)	Li(3B)	1.921(5)	N(3B)	Li(1B)	1.941(5)
N(3B)	Li(3B)	1.925(5)	N(2B)	Li(2B)	1.945(5)
N(4B)	Li(3B)	1.929(5)	N(4B)	Li(2B)	1.919(5)
O(1B)	Li(1B)	1.966(5)	O(3B)	Li(2B)	1.953(6)
O(2B)	Li(1B)	1.944(5)	O(4B)	Li(2B)	1.939(6)

Symmetry codes: (i) x, y, z; (ii) -x, y+1/2, -z+1/2; (iii) -x, -y, -z; (iv) x, -y-1/2, z-

1/2

Table A1.3: Selected bond angles (°) Structures A & B

Cl2 Cu1 Cl1	178.29(5)	Cl3 Cu2 Cl4	178.61(5)
Li3A N1A Li1A	86.5(2)	Li3B N1B Li1B	86.5(2)
Li2A N2A Li3A	87.7(2)	Li2B N2B Li3B	86.1(2)
P1A N1A Li3A	122.25(17)	P1B N1B Li3B	120.02(17)
P2A N2A Li3A	121.75(18)	P2B N2B Li3B	121.49(18)
P1A N1A Li1A	136.46(19)	P1B N1B Li1B	138.73(19)
P2A N2A Li2A	136.6(2)	P2B N2B Li2B	139.94(19)
N3A Li1A N1A	92.4(2)	N3B Li1B N1B	92.9(2)
N3A Li3A N1A	93.2(2)	N3B Li3B N1B	93.3(2)
N2A Li2A N4A	92.9(2)	N2B Li2B N4B	93.4(2)
N2A Li3A N4A	92.8(2)	N2B Li3B N4B	93.8(2)
N2A Li3A N1A	105.6(2)	N2B Li3B N1B	105.5(2)
N3A Li3A N4A	103.6(2)	N3B Li3B N4B	105.4(2)